

Non-Equilibrium Chemical Reactions Under Non-Isothermal Conditions: Kinetic Stabilization, Selection and Thermophoresis

Master Project
Section of Physics
École Polytechnique Fédérale de Lausanne

Author:

Shiling Liang

Supervisors:

Prof. Paolo De Los Rios
Dr. Daniel Maria Busiello

Lausanne, EPFL, 2020

The logo of the École Polytechnique Fédérale de Lausanne (EPFL), consisting of the letters 'EPFL' in a bold, red, sans-serif font.

Abstract

Life is likely to originate from non-equilibrium conditions. In the deep sea hydrothermal vents of the primitive earth, the presence of a temperature gradient and rich chemical components provided an ideal condition for the emergence of life. Before the formation of protocells, abiotic synthesis must take place and molecules evolve step by step to self-replicating molecules, a process also known as chemical evolution. This process is not likely to happen under an equilibrium condition since the chemical evolution is from stable inorganic components to thermodynamically unstable, complex self-replicating polymers. A temperature gradient can play the role as a non-equilibrium driven force to bring the prebiotic chemical evolution in non-equilibrium steady-state (NESS). In this thesis, we present a master equation description of non-equilibrium chemical reactions with Kramers-like transition rates. We use two simple reaction models to illustrate how chemical reaction systems utilize the non-isothermal environment to gain negative entropy and develop into kinetic-stable states. We also show that a periodic variation of temperature, as a stochastic pump, can drive the same reaction systems out of equilibrium to mimic the NESS. At last, we proposed a new mechanism of thermophoresis, a temperature gradient-driven inhomogeneous distribution of particles, based on a multi-state particle model with state-dependent diffusivity.

Key words: non-equilibrium thermodynamics, origin of life, stochastic thermodynamics, non-isothermal condition, kinetic stabilization, thermophoresis

Acknowledgements

I would like to express my deepest appreciation to Prof. De Los Rios for designing this interesting project and extraordinary support and in the past two year. And equiventaly my great appreciate to Dr. Busiello for inspiring discussions and patient instruction.

*I prefer using Chinese language to express my thanks to my parents:

谢谢我的父母在我在家写论文的这段时间给了我一个安心的环境, 以及在我成长过程中对我自由探索的支持与鼓励。

Chongqing, 19 June 2020

Shiling Liang | 梁师翎

Contents

List of figures	vii
1 Introduction	1
2 Non-equilibrium systems	3
2.1 From Newton equation to Langevin equation	3
2.2 From Langevin equation to Fokker-Planck equation	5
2.3 From Fokker-Planck equation to Master equation	7
2.4 Non-isothermal condition	10
2.4.1 Temperature gradient	10
2.4.2 Time-periodic temperature	11
2.5 Entropy production	12
3 Temperature gradient driving non-equilibrium chemical reaction	15
3.1 Large diffusion approximation	15
3.2 General analytic solution for two simple chemical reaction networks	16
3.2.1 States on a chain	16
3.2.2 Chemical states on a circle	17
3.3 Approximation methods	18
3.3.1 Perturbation theory	18
3.3.2 Two thermal reservoirs approximation	19
3.4 Two-state system: stabilization of high energy state	19
3.4.1 Stabilizing in large diffusion limit	19
3.4.2 Entropy production rate	22
3.5 Three-state system: dissipation-driven selection	23
3.5.1 Selection in large-diffusion limit	23
3.5.2 Optimal temperature for selection of three-state system	25
3.5.3 Entropy production	27
3.6 Autocatalysis	28
3.6.1 The mechanism of autocatalysis	28
3.6.2 Three-state selection with autocatalysis	29
3.6.3 Analytic solution in the large diffusion regime	30
3.6.4 Small diffusion - autocatalysis can either boost or suppress the selection	31

4	Time-periodic temperature driving non-equilibrium chemical reactions	33
4.1	Master equation with time-dependent transition rates	33
4.1.1	Near-equilibrium approximation	34
4.1.2	Zeroth-order and First-order solution	34
4.1.3	Second order equation	36
4.2	Three-state system and the dissipation-driven selection	37
4.2.1	Entropy production	38
4.3	Physical interpretations and applications	38
4.3.1	Chemical reactions in convection current	38
4.3.2	Reaction systems coupled to small reservoirs	39
5	Thermophoresis	41
5.1	Introduction	41
5.2	Spatially dependent diffusion coefficient	42
5.3	Multiple-state particle in temperature gradient	43
5.3.1	Multi-state particle	43
5.3.2	Particle with single chemical-state	47
5.3.3	Negative Soret coefficient due to particle-particle interaction	48
6	Conclusion	51
A	Appendixes	53
A.1	Derivation of Langevin equation	53
	Bibliography	59

List of Figures

2.1	A detailed view and a coarse-grained view of a large molecule in solvent. The solvent molecules collide with a large molecule to make it as a whole experience Brownian motion and its components experience constrained Brownian motion.	4
2.2	Dimension reduction of the chemical space. The free energy landscape is obtained by projecting the energy landscape to the reaction coordinate.	5
2.3	Energy landscape of a bistable reaction. The two local minimums can be regarded as discrete states. Then the transition rates between these two states can be calculated and referred as Kramers rate.	8
3.1	A two-state chemical reaction system in two boxes with different temperatures.	20
3.2	a. The NESS-triggered kinetic stabilizing effect for varying energy barriers varies with the energy barrier. b. The NESS stabilizing varies with temperature difference.	21
3.3	a. The energy landscape of a three-state system. b. The selection strength $R_{CB} \equiv P^{SS}(C)/P^{SS}(B)$	24
3.4	Contour plots of the selection strength, R_{CB} , for small energy difference and large energy difference.	25
3.5	a. Unbalance between $P(C)$ and $P(B)$ as a function of temperature difference. The three-state reaction system is coupled to two thermal reservoirs with temperature $T_1 = T - \Delta T$ and $T_2 = T + \Delta T$. The unbalancing is maximized around $\Delta T^* = 2T^2/(\epsilon_C + \epsilon_B)$, i.e. the middle between the perturbative regime and non-perturbative regime. b. The perturbative regime and non-perturbative regime. For a small temperature difference, called the perturbative regime, the selection strength grows quadratically with ΔT . In the non-perturbative regime (but still $\Delta T/T \ll 1$), the high-temperature transition rates dominate and abolish the selection when ΔT gets larger.	27
3.6	a. The energy transition state AA and AB can be eliminated to find the coarse-grained autocatalysis energy landscape. b. The energy barriers of both sides are lowered by an amount of δ in an autocatalytic reaction.	28
3.7	A comparison of selection strength of direct-transition reaction and autocatalytic reaction.	29
3.8	Autocatalysis can boost selection even when it does not change the kinetic barriers.	31
3.9	Autocatalysis can suppress selection when the diffusion coefficient is very small.	32

4.1	Numerical and perturbative solution of selection strength of the three-state system in periodic temperature with parameters $\beta_0 = 1$, $\beta_1(t) = \sin \omega t$, $\omega = 2\pi$, $\Delta E = 1$, $\varepsilon_C = 0.3$, $\varepsilon_B = 0.1$	37
5.1	a. Contour plot of the energy landscape of a six-state chemical reaction network, the local minimums (potential wells) can be regarded as discrete states. b. When the ensemble covariance of energies and diffusion coefficients of states are positive, the Soret coefficient is positive so that the particles accumulate on the cold side. c. For the negative covariance, the particle has a negative Soret coefficient and tend to stay on the hot side	44
5.2	The energy landscape of the binding and unbinding states. Dimers diffuse slower than monomers since the effective radius is larger.	48

1 Introduction

Living systems operate away from thermodynamics equilibrium, continually consuming energy[1]. Such a process is referred to as "feeds on negative entropy" by Schrödinger in his landmark book, *What is Life?*[2]

How can living systems emerge from the inanimate state? As we know, one key feature of living systems is that they can replicate themselves using building blocks; for example, RNA and DNA can use nucleotides to implement template replication. As RNA and DNA are not thermodynamically stable molecules, the replication must take place under non-equilibrium conditions. Furthermore, to initiate such a self-replicating process, spontaneous polymerization from abundant building blocks is required. The abundance of building blocks, such as nucleotides and amino acids (building blocks of proteins), cannot occur automatically but requires an externally driving force. It is believed that submarine hydrothermal vents of primitive earth are likely to be the place where the early life originated[3, 4]. The hot vent can provide essential chemical components and a temperature gradient as a driving force on chemical evolution. Thus we need to study the chemical reactions in non-isothermal conditions to see how prebiotic molecules can utilize the non-isothermal environment to evolve to higher-energy states for later use of polymerization, and how the non-isothermal environment leads to the accumulation of particles for more effective abiotic synthesis.

In the book *What is Life?*, Schrödinger also argues that the living organism avoids decaying "by eating, drinking, breathing and (in the case of plants) assimilating. The technical term is metabolism." However, in the very early stage of the origin of life, when neither protocells nor the metabolic cycles have formed, chemical evolution requires other sources of negative entropy. Stockar et al.[5] proposed that generating heat is another way to rid internal entropy production for microbial growth. Indeed, the increasing entropy of the environment due to heat exchange can also be interpreted as a negative entropy flux to the reaction systems. In the presence of a temperature gradient, the molecules absorb heat in the high-temperature region and expel this heat to the low-temperature reservoir, generating a steady negative entropy flow. The negative entropy flow brings the reaction system into an out-of-equilibrium state and allows it to explore a larger chemical space.

Now we need to find a proper theory to describe the chemical reaction in non-isothermal conditions. Various investigations on stochastic thermodynamics under non-isothermal conditions have been conducted[6–8]. In this manuscript, we follow a self-contained method to find master equations with transition rates of Kramers form to describe non-isothermal reactions. As derived step by step in Chapter 2, Kramers transition rates contain kinetic barriers, and as discussed in several studies[9–13], the kinetic features of a system provide another stabilization mechanism, called kinetic stabilization, which is distinct from the minimization of free energy of thermodynamic stabilization.

Unlike in the equilibrium case where thermodynamic stabilization results in the system's lowest free-energy state, in NESS conditions, a reaction system can be stabilized in states identified by its kinetic feature. This is in Chapter 3, where we illustrate that a temperature gradient can make a reaction system stabilize itself in its high-energy state. We also demonstrated that the higher the kinetic barrier is, the better the stabilization effect. Furthermore, a three-state reaction system, in which two low-energy states have equal energy but different kinetic barriers to the high-energy state, exhibits so-called dissipation-driven selection[14]. In both cases, the NESS is maintained by dissipation energy in a temperature gradient. By calculating the entropy production rates, we show that there are always negative entropy fluxes from the non-isothermal environment to the reaction system.

A NESS can be mimicked by a time-periodic variation of external driving parameters, namely a stochastic pump[15]. In Chapter 4, we show that the NESS of a reaction system in a temperature gradient can be mimicked by a periodic variation of temperature, such that the time-averaged quantities show the same behavior as the NESS quantities of the temperature gradient scenario.

The effect of temperature-gradient driven accumulation of particles called thermophoresis is also discussed, which is crucial in the origins of life since it can lead to an increase in the reactivity of polymerization[16, 17]. In Chapter 5, based on a multi-state particle model with state-dependent diffusivity, we propose a microscopic mechanism of thermophoresis and give an expression of the Soret coefficient which characterizes the strength of thermophoresis.

2 Non-equilibrium systems

In order to understand a chemical reaction system in non-isothermal conditions, we need first to know how to describe it. Here we start from classical mechanics and by integrating out all environment parameters to obtain a stochastic mechanics description. Then from the stochastic mechanics, we draw a probabilistic description, called the Fokker-Planck equation. Since chemical reactions describe transitions among discrete states and the potential energy landscape thus have several local minimums. The Fokker-Planck equation in a continuous chemical space can be further simplified to a discrete state master equation via the separation of timescale.

The non-isothermal condition will be introduced at the level of a discrete chemical reaction. The transition rates between states are temperature-dependent, so a non-isothermal condition, such as a temperature gradient or time-periodic variation of temperature, can maintain a reaction system out of equilibrium.

2.1 From Newton equation to Langevin equation

The first step is to derive the Langevin equation from a Hamiltonian system. Let us consider a system of a large molecule and its surrounding solvent molecules. The Hamiltonian of such a system can be separated into three terms, the large molecular part, the interaction part, and the environmental (solvent) part. The configuration of the large molecule can be represented by a set of coordinates of its n components in the position and momentum space, $\mathbf{p} = [p_1, p_2, \dots, p_n]$ and $\mathbf{q} = [q_1, q_2, \dots, q_n]$. For example, a polymer can be represented by the coordinate and the momentum of the constituting monomers.

$$\mathcal{H}(\mathbf{q}, \mathbf{p}, \mathbf{q}^e, \mathbf{p}^e) = H(\mathbf{q}, \mathbf{p}) + H_{env}(\mathbf{q}^e, \mathbf{p}^e) + H_{int}(\mathbf{q}, \mathbf{q}^e). \quad (2.1)$$

There are several solvable models proposed to derive the Langevin equation of Brownian particles from a Hamiltonian system[18, 19]. The main approximation is treating the solvent

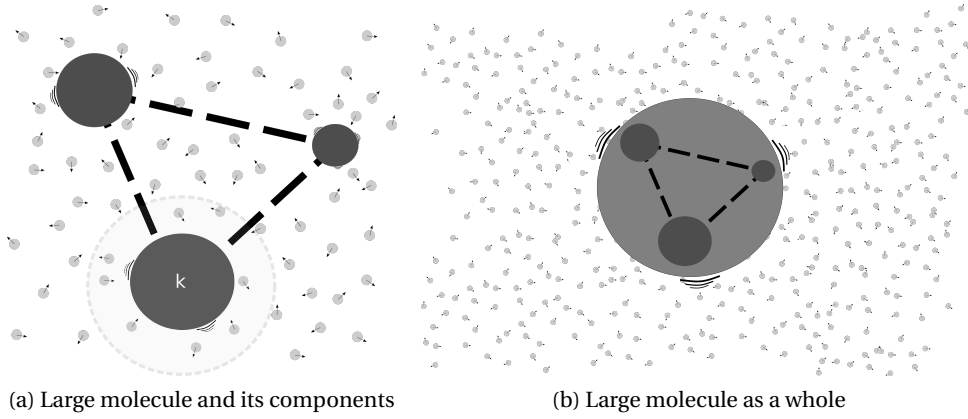


Figure 2.1 – A detailed view and a coarse-grained view of a large molecule in solvent. The solvent molecules collide with a large molecule to make it as a whole experience Brownian motion and its components experience constrained Brownian motion.

molecules as harmonic oscillators coupled to the Brownian particle. As the solvent molecules are much smaller than the Brownian particle, we can integrate out the solvent molecules by taking them as fast variables.

A component of the large molecule can be regarded as a constrained Brownian particle where the constrain is its interaction with the rest of the large molecule. Based on this, we can extend the derivation of Zwanzig[19] and obtain the over-damped Langevin equation of the k -th component of the large molecule (see detailed derivation in Appendix A.1)

$$\frac{dq_k}{dt} = -\frac{1}{\gamma_k} \partial_{q_k} U(\mathbf{q}) + \Gamma_k(t), \quad (2.2)$$

where $U(\mathbf{q})$ is the potential energy of the large molecule, γ_k is the friction coefficient of the k -th component and $\Gamma_k(t)$ is a white noise acting on j -th component of the particle. The noise and friction coefficient obeys fluctuation-dissipation theorem $\langle \Gamma_k(t) \Gamma_k(t') \rangle = \delta(t - t') k_B T / \gamma_k$.

The motion of the large molecule as a whole can be obtained by a direct weighted sum of the motion of its components where the weights are the sizes of the components, $\{s_k\}$. Note that the friction coefficient γ_k is proportional to the size s_k , hence we get

$$\frac{dx}{dt} = \frac{1}{s_k} \sum_k \frac{d(s_k q_k)}{dt} = \frac{1}{\sum_k \gamma_k} \sum_k \frac{d(\gamma_k q_k)}{dt} = \frac{1}{\sum_k \gamma_k} \sum_k \gamma_k \Gamma_k(t) = \Gamma'(t). \quad (2.3)$$

From this, we can define the friction coefficient for the large molecule as $\gamma_x = \sqrt{\sum_k \gamma_k^2 (\sum_k \gamma_k)^2}$, and collect the prefactor in the noise as diffusion coefficient $D_x = \frac{k_B T}{\gamma_x}$, we get the Langevin

equation in positional space as

$$\frac{dx}{dt} = \sqrt{2D_x}\eta_x(t). \quad (2.4)$$

Now we can study the Langevin equation for the chemical space. The chemical space has many degrees of freedom which are not all of the interests. Therefore we need to integrate out the unimportant degree of freedom and the remained ones are called the reaction coordinates. Fig.2.2 shows a simple example where the system has two degrees of freedom, but the transitions between potential wells happen along one direction. Thus, we can project the potential energy surface to the principle direction of reaction and obtain a one-dimensional free energy landscape, as shown in Fig. 2.2. Using q to denote the reaction coordinate, the Langevin equation on the free energy landscape reads

$$\frac{dq}{dt} = -\frac{1}{\gamma} \frac{dU(q)}{dq} + \sqrt{2D_q}\eta_q(t). \quad (2.5)$$

Here we use the potential energy $U(q)$ instead of free energy $G(q)$ is because when the temperature (noise) is much smaller than the energy barrier, the entropic part of the free energy is negligible so that $G \simeq E$, and the energy can be well-approximated by the potential energy $U(q)$ in the over-damped limit. Now the system is described by two Langevin equation: Eq. 2.4 describes the diffusion in positional space, and Eq. 2.5 describe the diffusion on the reduced chemical space - the reaction coordinate. These two Langevin equations generate stochastic trajectories in the position-chemical space.

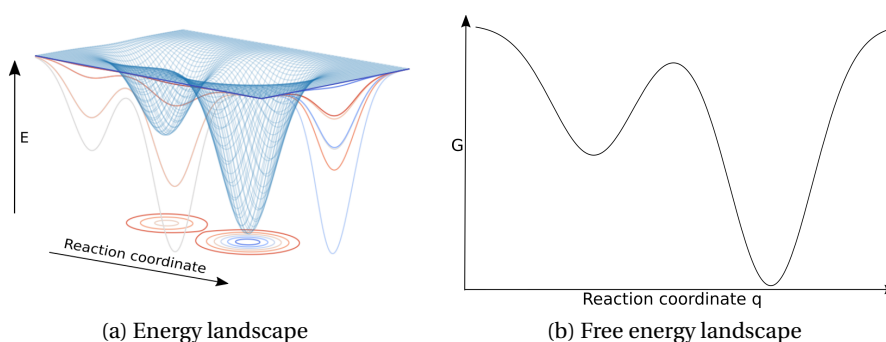


Figure 2.2 – Dimension reduction of the chemical space. The free energy landscape is obtained by projecting the energy landscape to the reaction coordinate.

2.2 From Langevin equation to Fokker-Planck equation

In the last section, we obtained an overdamped Langevin equation in the position-chemical space. These two equations generate stochastic trajectories of a particle in position-chemical

space. For many particles in a solvent system, what we observe is not an individual trajectory, instead, it is the statistical quantities such as concentration, or probability distribution. Therefore, if we can know the probabilities evolution governed by the Langevin equation, we can understand the behavior of the system.

To do so, we need to translate the trajectory description to the probabilistic description, namely the Fokker-Planck equation, which predicts the time-evolution of the probability distribution of a stochastic process. The derivation can be found in almost all standard textbooks of stochastic process[20–22]. Here we provide a short version to capture the main steps of the derivation.

For a stochastic process described by Langevin equation

$$\dot{x} = A(x) + B(x)\eta(t), \quad (2.6)$$

the mean and average of the increment of the stochastic variable in a short time interval Δt can be calculated using Ito calculus as

$$\begin{aligned} \langle \Delta x \rangle_{\Delta t} &= A(x)\Delta t \\ \langle \Delta x^2 \rangle_{\Delta t} &= B^2(x)\Delta t. \end{aligned} \quad (2.7)$$

Then we are interested in the evolution equation of probability $P(x, t)$. It can be expressed by the Chapman-Kolmogorov equation as

$$P(x, t + \Delta t) = \int_{x_0} dx_0 P(x, t + \Delta t | x_0, t) P(x_0, t). \quad (2.8)$$

We can expand the conditional probability to the second order of Δt

$$P(x, t | x_0, t - \Delta t) = \delta(x - x_0) + \langle \Delta x \rangle_{\Delta t} \partial_x \delta(x - x_0) + \frac{1}{2} \langle \Delta x^2 \rangle_{\Delta t} \partial_x^2 \delta(x - x_0). \quad (2.9)$$

Substituting it back to Eq. 2.8 gives

$$P(x, t + \Delta t) = P(x, t) + \partial_x (\langle \Delta x \rangle P(x, t)) + \frac{1}{2} \partial_x^2 (\langle \Delta x^2 \rangle P(x, t)). \quad (2.10)$$

The mean and average are related to the drift, and noise terms are given in Eq. 2.7. Therefore we obtain the time evolution equation of the probability distribution of the stochastic variable x

$$\partial_t P(x, t) = \partial_x (A(x)P(x, t)) + \frac{1}{2} \partial_x^2 (B(x)^2 P(x, t)). \quad (2.11)$$

For the chemical reaction system of interest, we have two Langevin equations. The corresponding Fokker-Planck equation in the position-chemical space is

$$\partial_t P(x, q, t) = \partial_x^2 (D_x P(x, q, t)) - \partial_q \left(-\frac{1}{\gamma_q} P(x, q, t) \partial_q U(q) \right) + \partial_x^2 (D_q P(x, q, t)). \quad (2.12)$$

2.3 From Fokker-Planck equation to Master equation

Chemical reactions are defined on a set of discrete states, describing transition among some chemical species. That means we need to do one more step to find well-defined states from a continuous energy landscape in chemical space. In thermodynamic equilibrium, a system described by the Fokker-Planck equation relaxes to Boltzmann distribution. The exponential nature of Boltzmann distribution guarantees that the system mainly stays in the local minimums of the energy landscape. That means the chemical space can be well-discretized by regarding the local minimums of potential as discrete chemical states. Therefore, we can construct a master equation to describe the transitions among the potential wells based on the Fokker-Planck equation.

Let us consider a bistable system as an example. As shown in Fig. 2.3, the chemical space is one-dimensional, and the energy landscape has two local minimums. When the temperature is low enough, the particles mainly stay in two potential wells. Labeling the two wells as state A and B . A particle in either state can gain thermal energy from the environment and jump across the barrier to reach the other state, so we have a two-state chemical reaction $A \rightleftharpoons B$ and the time-evolution of the probability distribution is described by a master equation:

$$\begin{aligned} \partial_t p_A &= -k_{BA} p_A + k_{AB} p_B \\ \partial_t p_B &= -k_{AB} p_B + k_{BA} p_A, \end{aligned} \quad (2.13)$$

The two transition rates k_{BA} and k_{AB} need to be derived from the Fokker-Planck equation. The first step is to rewrite Eq. 2.12 in form of fluxes in the position-chemical space:

$$\partial_t P + \partial_x J_x + \partial_q J_q = 0 \quad \text{where} \quad \begin{cases} J_x = -\partial_x (D_x P) \\ J_q = -P \frac{1}{\gamma} \partial_q H - \partial_q (D_q P). \end{cases} \quad (2.14)$$

The flux in the q direction can be written in a compact form:

$$J_q = -D_q e^{-\frac{H}{k_B T}} \partial_q \left(e^{\frac{H}{k_B T}} P \right), \quad (2.15)$$

where we used the Stokes-Einstein relation $D_q = k_B T / \gamma_q$. The escape rate was first derived by Kramers, hence it is called Kramers escape rate, which is defined by the ratio of the escape flux

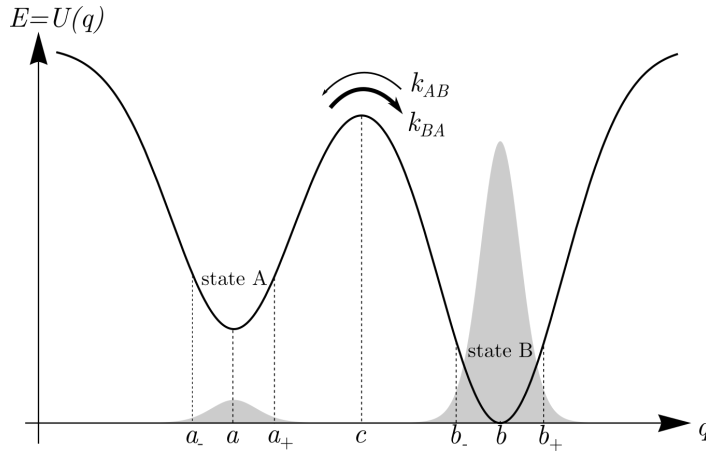


Figure 2.3 – Energy landscape of a bistable reaction. The two local minimums can be regarded as discrete states. Then the transition rates between these two states can be calculated and referred as Kramers rate.

from one state and the probability in that state:

$$k_{BA} \equiv \frac{J_{ba}}{p_A} \quad (2.16)$$

So to find the Kramers rate from state A to B, we need to calculate both the probability in state A and the flux. To find the flux J_{ba} , let us rewrite the Eq. 2.15 as

$$\frac{J_q}{D_q e^{-\frac{U}{k_B T}}} = -\partial_q \left(e^{\frac{U}{k_B T}} P \right). \quad (2.17)$$

Suppose the system relaxes to near-equilibrium in state A and is empty in state B, the flux is purely from the potential well A so that $J_q = J_{ba}$. The near-equilibrium ensures that J_q is independent of q , which allows us to integrate both sides of the above equations from a to b :

$$\begin{aligned} J_{ab} &= \frac{-D_q e^{\frac{U}{k_B T}} P|_a^b}{\int_a^b e^{\frac{U}{k_B T}} dq} = \frac{D_q e^{\frac{U(a)}{k_B T}} P(a)}{\int_a^b e^{\frac{U}{k_B T}} dq} && \leftarrow P(b)=0 \\ &\simeq \frac{D_q e^{\frac{U(a)}{k_B T}} P(a)}{\int_a^b \exp \left[\frac{1}{k_B T} \left(U(c) + \frac{1}{2} U''(c) (q-c)^2 \right) \right] dq} && \leftarrow \text{saddle point approximation around } c \\ &\simeq D_q \sqrt{\frac{|U''(c)|}{2\pi k_B T}} e^{-\frac{U(c)-U(a)}{k_B T}} P(a). \end{aligned} \quad (2.18)$$

The flux is obtained, then we need to calculate the probability in state A , i.e. the probability of the particle's state in the region $[a_-, a_+]$. The local-equilibrium condition in potential well A gives the relation $P(q)/P(A) = \exp(-(U(q) - U(A))/k_B T)$. Plugging it into the integral gives

$$\begin{aligned}
 p_A &= \int_{a^-}^{a^+} P(q) dq = \int_{a^-}^{a^+} P(a) e^{-\frac{U(q)-U(a)}{k_B T}} dq && \leftarrow \text{Local-Boltzmann} \\
 &\simeq \int_{-\infty}^{\infty} P(a) e^{-\frac{U''(a)(q-a)^2}{2k_B T}} dq && \leftarrow \text{saddle-point approximation around } a \\
 &= P(a) \sqrt{\frac{2\pi k_B T}{|U''(a)|}}.
 \end{aligned} \tag{2.19}$$

Using the definition of the Kramers escape rate, we finally obtain the transition rate from state A to state B :

$$\begin{aligned}
 k_{BA} &\equiv \frac{J_{ba}}{p_A} = D_q \frac{1}{2\pi k_B T} \sqrt{|U''(a)U''(c)|} \exp\left[-\frac{U(c) - U(a)}{k_B T}\right] \\
 &= \frac{1}{2\pi\gamma_q} \sqrt{|U''(a)U''(c)|} \exp[-U(c) - U(a)k_B T].
 \end{aligned} \tag{2.20}$$

The escape rate in the opposite direction can be derived in the same fashion and is

$$k_{AB} = \frac{1}{2\pi\gamma_q} \sqrt{|U''(b)U''(c)|} \exp\left[-\frac{U(c) - U(b)}{k_B T}\right]. \tag{2.21}$$

These two rates characterize the reaction dynamics between these two states. The transition rates in Kramers form contain two parts. One is a reaction constant $k_0 = \frac{1}{2\pi\gamma_q} \sqrt{|U''(a)U''(c)|}$ only depends on the shape of the curvature of the potential at the point a and c . The other part, $\exp[-(U(c) - U(a))/k_B T]$ falls exponentially with the activation energy to cross the barrier.

The prefactors of the transition rate, $f(a) = \sqrt{|U''(a)U''(c)|}$ and $f(b) = \sqrt{|U''(b)U''(c)|}$ are not the same and will lead to the non-Boltzmann ratio between the two chemical states

$$\frac{p_a}{p_b} = \frac{k_{AB}}{k_{BA}} = \sqrt{\frac{U''(b)}{U''(a)}} e^{-\frac{U_a - U_b}{k_B T}}. \tag{2.22}$$

This non-Boltzmann contribution comes from the unfair definition of two discrete states around the local minimums. The two potential wells have different characteristic widths, which are proportional to $\sqrt{1/U''(a)}$ and $\sqrt{1/U''(b)}$, respectively. Therefore, in order to make a fair definition of 'state', we should seek for states in different regions of the same width. Thus,

the probabilities on each state should be corrected as

$$p_A \rightarrow W \sqrt{U(a)''} p_A, \quad p_B \rightarrow W \sqrt{U(b)''} p_B. \quad (2.23)$$

where W is a constant which characterizes the width of each state. Using \mathcal{E}_{BA} to denote the activation energies of transitions, the reaction rates can be written as

$$k_{AB} = k_0 \exp\left(-\frac{\mathcal{E}_{AB}}{k_B T}\right) \quad k_{BA} = k_0 \exp\left(-\frac{\mathcal{E}_{BA}}{k_B T}\right). \quad (2.24)$$

Now the ratio between the two reaction rates only depends on the energy difference. We can further extend the two-state system to a complex reaction network, containing a set of states $\{C_i\}$. The transition rate from state C_i to C_j is $k_{C_j C_i} = k_0 \exp(-\mathcal{E}_{C_j C_i} / k_B T)$. Under this scheme, the time-evolution equation of the chemical reaction network is a master equation

$$\partial_t p_{C_i} = \sum_{j \neq i} (k_{C_i C_j}(T) p_{C_j} - k_{C_j C_i}(T) p_{C_i}). \quad (2.25)$$

In the equilibrium case, a reaction system is coupled to a single thermal reservoir and the corresponding stationary state is the thermodynamic equilibrium state, whose probability distribution is given by Boltzmann distribution. And any quantity of interest can be calculated using the standard method of classical thermodynamics. Now if we put the system in an inhomogeneous environment, such as a temperature gradient, the system is then brought out of equilibrium. There does not exist a standard method to solve such a non-equilibrium system, and studying such a non-equilibrium chemical reaction system is the main theme of this thesis.

2.4 Non-isothermal condition

After preparing mathematical tools to describe chemical reaction systems, we can now introduce the non-isothermal condition to bring this system out of equilibrium. There are two ways to implement a non-isothermal condition, one is a temperature gradient, and the other is a time-dependent temperature.

2.4.1 Temperature gradient

For the spatial non-equilibrium, the particles can diffuse in positional space which is coupled to a temperature gradient. The consequence evolution equation is thus a reaction-diffusion equation. Supposing the particle has a set of state $\{C_i\}$ and the reaction in the chemical space

is described by a master equation, then the evolution equation is given by

$$\partial_t p_{C_i}(x, t) = \sum_{j \neq i} (k_{C_i C_j}(x) p_{C_j}(x, t) - k_{C_j C_i}(x) p_{C_i}(x, t)) + D_{C_i} \nabla^2 p_{C_i}(x, t). \quad (2.26)$$

The transition rates $k_{C_i C_j}(x) = k_0 \exp(-\mathcal{E}_{C_i C_j} / T(x))$ is a function of position comes from the fact that it is temperature dependent and there is a temperature gradient along x . In a non-equilibrium steady state (NESS), the system relaxed to a unique time-independent state, we can find some interesting features due to its non-equilibrium nature. Two quantities need to be calculated, the first one is the total probability in state C_i , defined as

$$P(C_i) = \int_0^L p_{C_i}(x) dx, \quad (2.27)$$

where the integral runs over the whole position space and gives us the total probability of the state C_i . Unlike in thermodynamic equilibrium, where this probability is solely determined by the state variable - the energies of the state, where we need to also include the kinetic character of the system. In the next chapter, we will have a detailed discussion on the properties of a NESS and how it compares to the thermodynamic equilibrium state.

The second quantity of interest is the non-uniform distribution of all particles, characterized by boundary

$$p_{tot}(x) = \sum_i p_{C_i}(x). \quad (2.28)$$

This non-uniform distribution is namely the thermophoresis effect that a temperature gradient induces a concentration gradient in a diffusion system. We will show how this effect emerges from a multi-state particle model when different states have different diffusion coefficients in Chapter 5.

2.4.2 Time-periodic temperature

The second type of non-isothermal condition is a time-dependent temperature coupled to reaction systems. The master equation for this case reads

$$\partial_t p_{C_i}(t) = \sum_{j \neq i} (k_{C_i C_j}(t) p_{C_j}(t) - k_{C_j C_i}(t) p_{C_i}(t)). \quad (2.29)$$

As the temperature is time-dependent, the transition rate $k_{C_i C_j} = \exp(-\mathcal{E}_{C_i C_j} / T(t))$ also varies in time. Supposing a periodic variation of temperature with period τ , then we can define a

time-average probability in state C_i as

$$P(C_i) = \overline{P_{C_i}} = \frac{1}{\tau} \int_{t_0}^{t_0+\tau} p_{C_i}(t) dt. \quad (2.30)$$

In Chapter 4, we will show these time-averaged quantities are analogies to the space-average defined by Eq. 2.27.

2.5 Entropy production

A key feature of a non-equilibrium system is that the entropy production is non-zero. For a master equation, Schnakenberg's entropy production rate reads

$$\dot{S} = \frac{1}{2} \sum_{j \neq i} (J_{C_i C_j} - J_{C_j C_i}) \ln \left[\frac{J_{C_i C_j}}{J_{C_j C_i}} \right], \quad (2.31)$$

where $J_{C_i C_j} = k_{C_i C_j} p_{C_j}$ is the flux from state C_j to C_i . The entropy production rate can be separated into two terms. One is the entropy production inside the system, the other one is the entropy production rate in the environment due to the coupling of the system to thermal reservoir(s):

$$\begin{aligned} \dot{S}_{env} &= \frac{1}{2} \sum_{j \neq i} (k_{C_i C_j} p_{C_j} - k_{C_j C_i} p_{C_i}) \ln \left[\frac{k_{C_i C_j}}{k_{C_j C_i}} \right] \\ \dot{S}_{sys} &= \frac{1}{2} \sum_{j \neq i} (k_{C_i C_j} p_{C_j} - k_{C_j C_i} p_{C_i}) \ln \left[\frac{p_{C_j}}{p_{C_i}} \right]. \end{aligned} \quad (2.32)$$

One can easily verify the following relation:

$$\dot{S}_{sys} = \frac{d}{dt} \left(- \sum_i p_{C_i} \ln p_{C_i} \right), \quad \dot{S}_{env} = \frac{1}{2} \sum_{j \neq i} J_{C_j \rightarrow C_i} \frac{E_j - E_i}{T} = \frac{\dot{Q}}{T}. \quad (2.33)$$

where $J_{C_j \rightarrow C_i} = J_{C_i C_j} - J_{C_j C_i}$ is the net flux from state C_j to C_i . The heat flow directed from the system to the environment is defined as positive. From the above equations, we can see that the internal entropy production rate is the time derivative of Gibbs entropy ($k_B = 1$) of the system, and the entropy production of the environment is related to the heat exchange so we can interpretative it as thermodynamic entropy production.

Now we have the entropy production rate as the master equation in an arbitrary state. If the chemical reaction system is coupled to a single constant temperature reservoir, both \dot{S}_{sys} and \dot{S}_{env} will relax to zero when the system is in an equilibrium state. While we are interested in the NESS driven by temperature gradient or time-periodic temperature, in both cases we can

define the total entropy production rate, either over the whole gradient or averaged over one period of the time-dependent temperature.

For the temperature gradient case, the chemical reaction system reaches a NESS, so $\dot{S}_{sys} = 0$, and the entropy production only comes from the heat exchange between the system and the reservoirs, which gives the average as

$$\dot{S}^{ss} = \int_x dx \dot{S}_{env}(x) = \int_x dx \frac{\dot{Q}(x)}{T(x)} > 0. \quad (2.34)$$

As for the time-periodic temperature case, the internal entropy production over one period is zero, $\int_t^{t+\tau} dt \dot{S}_{sys} = S_{sys}(t+\tau) - S_{sys}(t) = 0$. So the net entropy production is also solely from the coupling of the system and the thermal reservoir. We can use the mean entropy production rate to characterize the dissipation of a time-periodic-driven system:

$$\bar{\dot{S}} = \frac{1}{\tau} \int_t^{t+\tau} dt \dot{S}_{env}(t) = \frac{1}{\tau} \int_t^{t+\tau} dt \frac{\dot{Q}(t)}{T(t)} > 0. \quad (2.35)$$

In both cases, the entropy production of the environment is positive, which means a NESS is maintained by increasing the environmental entropy. Alternatively, we can use entropy flux to understand this process. The positive entropy production rate in the environment is associated with a positive entropy flux from the system to the environment, or equivalently a negative entropy flux from the environment to the system:

$$J_S^{in} = -\dot{S}_{env} < 0 \quad (2.36)$$

This interpretation matches Schrodinger's statement, "life feeds on negative entropy"[2]. In Chapter 3 we will study two chemical reaction systems that are maintained in a NESS by feeding it with negative entropy.

3 Temperature gradient driving non-equilibrium chemical reaction

In this chapter, we study chemical reactions in temperature gradient and show how reaction systems maintain themselves in more organized states than equilibrium Boltzmann distribution via dissipating of energy.

We first adopt the large diffusion approximation to allow us to find the analytic solutions of non-equilibrium steady state (NESS) for two types of reaction networks. This approximation can also significantly simplify the perturbative solution. Then, two simple reaction systems are proposed for illustration of the effects of dissipating energy in a temperature gradient. The first is a two-state reaction system coupled to two thermal reservoirs with different temperatures. As reaction system can stabilize itself in the high energy state by increasing the entropy of the environment. Then we study a three-state system with kinetic asymmetry, which is also coupled to two thermal reservoirs, and shows that it can distinguish this kinetic asymmetry and show bias to two states with the same energy but involved in reactions with different dissipating rates. At last, we numerically explore the effect of autocatalytic reaction for the three-state dissipation-driven selection system.

3.1 Large diffusion approximation

For the non-isothermal reaction-diffusion equation proposed in chapter 2, diffusion and reaction compete with each other. If the diffusion coefficient is small enough, the steady-state of the system will reach a local-equilibrium state, and that local-Boltzmann distribution is obeyed. In the local equilibrium regime, the probability distribution among the states is trivially determined by the energies of states and the local temperature. In the opposite limit, that the diffusion is much faster than chemical reactions, the reaction system is effectively coupled to multiple thermal reservoirs simultaneously, and the transition rates are the direct average of the transition rates to each thermal reservoir.

Taking the limit $D_{C_i} \rightarrow \infty$, then the probability of staying in a specific state is constant along the temperature gradient, then we can integrate the equation over the whole position space to

find the evolution equation of the marginal distribution in the chemical space:

$$\partial_t P(C_i) = \sum_j \bar{k}_{C_i C_j} P(C_j). \quad (3.1)$$

The diffusion term vanished due to the no-flux boundary condition, and the transition rates here are the spatial average, namely $\bar{k}_{C_i C_j} = \frac{1}{L} \int_0^L k_{C_i C_j}(T(x)) dx$. Unlike the constant temperature case, under which the ratio of probabilities of two states is determined by energy difference, $P^{eq}(C_i)/P^{eq}(C_j) = \exp(-(E_i - E_j)/T)$, the topologies and the kinetics of the reaction network must be taken into account in the non-isothermal scenario. In the large-diffusion limit, the ratio between a pair of transition rates in opposite directions is

$$\frac{\bar{k}_{C_i C_j}}{\bar{k}_{C_j C_i}} = \frac{\int_0^L \exp(-\mathcal{E}_{C_i C_j}/T(x)) dx}{\int_0^L \exp(-\mathcal{E}_{C_j C_i}/T(x)) dx}, \quad (3.2)$$

where the activation barrier can not be eliminated, so in the non-equilibrium condition, the full kinetic features of the network are reflected in the NESS. Analytic solution of such a system can be obtained either by standard linear algebra method (Cramer's rule) or spanning-tree method[23, 24]. The solution obtained by Cramer's rule is not easy to find physical interpretations, while the spanning tree method needs to be calculated case by case for specific networks. Therefore we aim to find general analytical solutions for specific types of reaction networks and also a general approximation method for any network.

3.2 General analytic solution for two simple chemical reaction networks

Here we present types of chemical reaction networks for which general solutions are able to obtain. The first one is stated on a single chain, such that there is no loop in the large-diffusion coarse-grained level. The second type is the simplest loop case that all chemical states are on a cycle. Then in the rest of the paper, we can directly use the solutions obtained in this chapter.

3.2.1 States on a chain

Suppose we have n chemical states along a chain and the reaction can only take place between adjacent states, the evolution equation of such as system reads

$$\partial_t P(C_i) = \begin{cases} \bar{k}_{C_i C_{i+1}} P(C_{i+1}) + \bar{k}_{C_i C_{i-1}} P(C_{i-1}) - (\bar{k}_{C_{i+1} C_i} + \bar{k}_{C_{i-1} C_i}) P(C_i) & i \neq 0, n \\ \bar{k}_{C_0 C_1} P(C_1) - \bar{k}_{C_1 C_0} P(C_0) & i = 0 \\ \bar{k}_{C_n C_{n-1}} P(C_{n-1}) - \bar{k}_{C_{n-1} C_n} P(C_n) & i = n \end{cases} \quad (3.3)$$

Since there is no loop, the system always satisfies detailed balance conditions. Therefore, the probability in the state C_k can be calculated recursively from the probability in state C_0 as

$$P(C_k) = \frac{\prod_{i=1}^k \bar{k}_{C_i C_{i-1}}}{\prod_{i=1}^k \bar{k}_{C_{i-1} C_i}} P(C_0). \quad (3.4)$$

With the normalization condition, we obtain the probability in the state C_k as

$$P(C_k) = \frac{\prod_{i=1}^k \bar{k}_{C_i C_{i-1}}}{\prod_{i=1}^k \bar{k}_{C_{i-1} C_i} + \sum_{k=1}^n \prod_{i=1}^k \bar{k}_{C_{i-1} C_i}}. \quad (3.5)$$

It is worth noting that the system obeys detailed balance in the level of large-diffusion coarse-graining. If we take into account the diffusive flux along position space, the system still has loops. When we want to calculate other physical quantities such as entropy production rate, we need to go back to the reaction-diffusion picture and use Eq. 2.34.

3.2.2 Chemical states on a circle

The simplest reaction network with loops is a circle with states on it. Still supposing all chemical transitions can only happen between adjacent states, we have the evolution equation:

$$\partial_t P_{C_i} = \sum_{k=C_{i-1} C_{i+1}} (\bar{k}_{C_i C_k} P_{C_k} - \bar{k}_{C_k C_i} P_{C_i}). \quad (3.6)$$

All states are on a circle, so the periodic boundary condition applies, $i + n \equiv i$. Since there is only one single loop, only a constant flux exists along the cycle. Denoting the flux by J and setting the clockwise direction as positive, we then obtain the steady-state balance between two adjacent states:

$$J = -\bar{k}_{C_i C_{i+1}} P_{C_{i+1}} + \bar{k}_{C_{i+1} C_i} P_{C_i}. \quad (3.7)$$

With the above equation, one can get the ratio of P_{C_k} to P_{C_l} recursively:

$$P_{C_k} = P_{C_l} \prod_{i=l+1}^k \frac{\bar{k}_{C_i C_{i-1}}}{\bar{k}_{C_{i-1} C_i}} - J \sum_{m=l+1}^k \left[\frac{1}{\bar{k}_{C_{m-1}, C_m}} \prod_{i=m}^k \frac{\bar{k}_{C_i C_{i-1}}}{\bar{k}_{C_{i-1} C_i}} \right]. \quad (3.8)$$

Taking this calculation along a full cycle, thanks to the periodic boundary condition, we obtain

the relation between J and probability on state k as

$$J = \frac{\left(\prod_{i=k-n+1}^k \frac{\bar{k}_{C_i C_{i-1}}}{\bar{k}_{C_{i-1} C_i}} - 1 \right) P_{C_k}}{\sum_{m=k-n+1}^k \left[\frac{1}{\bar{k}_{C_{m-1} C_m}} \prod_{i=m}^k \frac{\bar{k}_{C_i C_{i-1}}}{\bar{k}_{C_{i-1} C_i}} \right]}. \quad (3.9)$$

The one-cycle product $\prod_{i=k-n+1}^k$ is independent of the starting point. For a system obeys detailed balance, $\prod_{i=k-n+1}^k \frac{\bar{k}_{C_i C_{i-1}}}{\bar{k}_{C_{i-1} C_i}} = 1$, hence the net flux J is zero. Substituting Eq. 3.9 to Eq. 3.8 gives the ratio of P_{C_k} to P_{C_l}

$$\frac{P_{C_k}}{P_{C_l}} = \frac{\sum_{m=k-n+1}^k \left[\frac{1}{\bar{k}_{C_{m-1} C_m}} \prod_{i=m}^k \frac{\bar{k}_{C_i C_{i-1}}}{\bar{k}_{C_{i-1} C_i}} \right]}{\sum_{m=l-n+1}^l \left[\frac{1}{\bar{k}_{C_{m-1} C_m}} \prod_{i=m}^l \frac{\bar{k}_{C_i C_{i-1}}}{\bar{k}_{C_{i-1} C_i}} \right]}. \quad (3.10)$$

3.3 Approximation methods

3.3.1 Perturbation theory

The perturbation theory is always a useful tool to get a good understanding of how is a system driven out from a solved model by external perturbation. Here the solved model is the equilibrium thermodynamic distribution of a reaction network coupled to a constant temperature thermal reservoir. The perturbation here is thus the coupled temperature gradient. Firstly, we need to define the equilibrium states of the system. As equilibrium thermodynamics is defined by a constant temperature and a set of energies, here the energies of states are fixed, what needs to find is the temperature. An intuitive choose is using the average temperature, $\bar{T} = \frac{1}{L} \int_L T(x) dx$, to find the thermodynamic equilibrium state. Therefore the perturbation to the temperature at position x is $\Delta T(x) = T(x) - \bar{T}$. Under the large diffusion limit, the time-scale in the x -direction can be eliminated as mentioned above, hence the perturbation needs to be integrated out along the position space. Then, we can expand the transition rate from the equilibrium rate of average temperature \bar{T} :

$$\begin{aligned} \bar{k}_{C_i C_j} &= \frac{1}{L} \int_L k_0 \exp \left[-\frac{\mathcal{E}_{C_i C_j}}{T(x)} \right] dx \\ &= \frac{k_0}{L} \int_L \exp \left[-\frac{\mathcal{E}_{C_i C_j}}{\bar{T} + (T(x) - \bar{T})} \right] \\ &= \frac{k_0}{L} \int_L \exp \left[-\frac{\mathcal{E}_{C_i C_j}}{\bar{T}} + \frac{\mathcal{E}_{C_i C_j}}{\bar{T}^2} \Delta T(x) + \mathcal{O}((\Delta T(x)/\bar{T})^2) \right] \\ &= k_{C_i C_j}(\bar{T}) \left(1 + \frac{\delta^2}{2} \frac{\mathcal{E}_{C_i C_j}^2}{\bar{T}^2} \right). \end{aligned} \quad (3.11)$$

where $\delta = \frac{\sqrt{\text{Var}(T)}}{\bar{T}}$. Then we expand steady-state distribution in powers of δ :

$$P^{ss}(C_i) = P^{eq}(C_i) + \delta^2 P_2(C_i). \quad (3.12)$$

The zeroth order term is the equilibrium distribution corresponding to the average temperature. The first-order term vanished since there is no first-order term in the expansion of transition rates, or physically we can say that a particle should not directly feel the direction of the temperature gradient. Therefore the perturbation on probabilities starts from the second order, i.e. the variance of the temperature.

The validity of perturbation theory A condition must be satisfied to do the expansion of the last line of Eq 3.11, that is $|\Delta T(x) \mathcal{E}_{C_i C_j} / \bar{T}^2| \ll 1$ for any x . So both the lowest and highest temperatures should satisfy this condition. Jointing these two requirements give

$$\frac{(T_{max} - T_{min}) \mathcal{E}_{C_i C_j}}{2\bar{T}^2} \ll 1. \quad (3.13)$$

3.3.2 Two thermal reservoirs approximation

Without loss of generality but with great simplicity, we study chemical reactions operating in two boxes coupled to two thermal reservoirs, one of temperature $T_1 = T - \Delta T$ and the other of temperature $T_2 = T + \Delta T$. The transport of a species between two boxes is diffusion-like, denoting by d_{C_i} for species C_i . The large diffusion coefficient here is $d_{C_i} \rightarrow \infty$, and the averaged transition rate is thus

$$\bar{k}_{C_i C_j} = \frac{1}{2} \left(k_0 e^{-\mathcal{E}_{C_i C_j} / (T - \Delta T)} + k_0 e^{-\mathcal{E}_{C_i C_j} / (T + \Delta T)} \right). \quad (3.14)$$

Under this scheme, the integration along a temperature gradient is replaced by summation. And the main features of the system, the non-isothermal condition, still remain. In the following sections, we will restrict ourselves to this two-box model and have a more transparent look at how a chemical reaction system responds to non-isothermal conditions.

3.4 Two-state system: stabilization of high energy state

3.4.1 Stabilizing in large diffusion limit

To understand how non-isothermal conditions change the probability distribution of a chemical reaction system, let us consider the simplest case, a two-state particle with a high energy state A and a low energy state B . The system can be brought out of equilibrium by coupling to multiple thermal reservoirs with different temperatures. Without loss of generality, we con-

sider the simplest setup that there are only two thermal reservoirs of temperature $T_1 = T - \Delta T$ and $T_2 = T + \Delta T$. consequently, the evolution equations for the two-box reaction system is

$$\begin{aligned}\partial_t P(A_i) &= -k_{B_i A_i} P(A_i) + k_{A_i B_i} P(B_i) + d_A (P(A_j) - P(A_i)) \\ \partial_t P(B_i) &= -k_{A_i B_i} P(B_i) + k_{B_i A_i} P(A_i) + d_B (P(B_j) - P(B_i)),\end{aligned}\quad (3.15)$$

where X_i denotes species X in box i , $\{i, j\} = \{1, 2\}$ or $\{2, 1\}$, the transition rates are of Kramers-form and d_X is the diffusion-like transport coefficient between two boxes for species X . The energy difference between two states is ΔE , the energy barrier from state A to B is $\mathcal{E}_{BA} = \varepsilon$ and consequently, the activation of the opposite direction is $\mathcal{E}_{AB} = \Delta E + \varepsilon$. In equilibrium condition of constant temperature T , the probability on the high energy state A is $P^{eq}(A) = 1/(1 + e^{-\Delta E/T})$, which contains no information about the kinetic barrier ε .

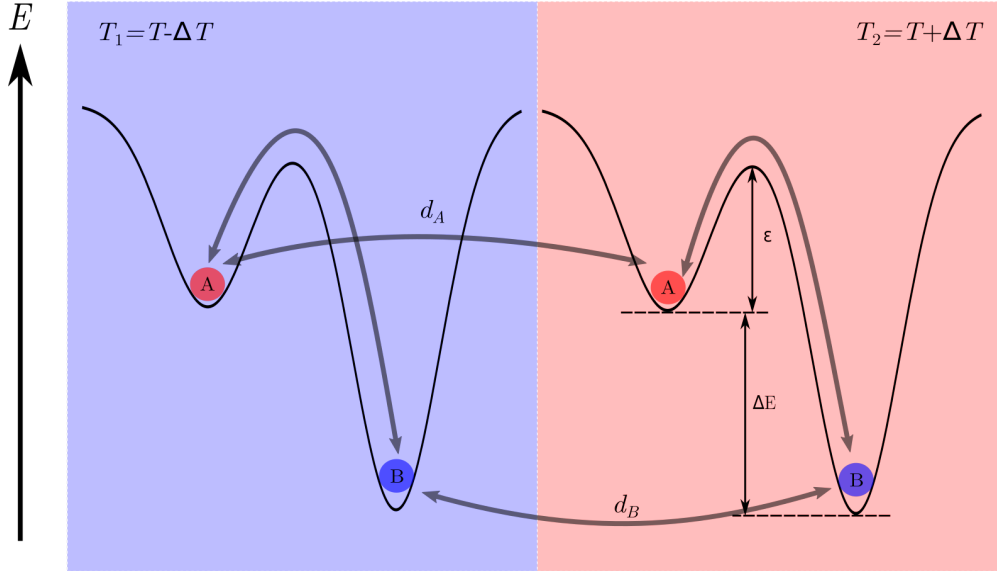


Figure 3.1 – A two-state chemical reaction system in two boxes with different temperatures.

While, in the large diffusion limit, $d_x \rightarrow \infty$, this master equation is reduced to Eq. 3.1. The non-equilibrium transition rates between these two states are the average of the rates in the two reservoirs:

$$\bar{k}_{AB} = \frac{1}{2} (e^{-(\Delta E + \varepsilon)/T_1} + e^{-(\Delta E + \varepsilon)/T_2}), \quad \bar{k}_{BA} = \frac{1}{2} (e^{-\varepsilon/T_1} + e^{-\varepsilon/T_2}). \quad (3.16)$$

Such a two-state chemical reaction network is the shortest chain model, so the solution is given by the general solution in Sec. 3.2.1. The steady-state probability on the high energy state A is given by

$$P^{ss}(A) = \frac{\bar{k}_{BA}}{\bar{k}_{BA} + \bar{k}_{AB}} = \frac{e^{-\varepsilon/T_1} + e^{-\varepsilon/T_2}}{e^{-\varepsilon/T_1} + e^{-\varepsilon/T_2} + e^{-(\Delta E + \varepsilon)/T_1} + e^{-(\Delta E + \varepsilon)/T_2}} > P^{eq}(A; T). \quad (3.17)$$

The NESS probability of a high energy state is always larger than that of the equilibrium distribution of average temperature T . So we can say that a temperature gradient can stabilize the reaction system in the high energy state. Based on the dynamics of the system, we can understand this stabilization effect as the high-temperature reservoir pumps the system to the high-energy state, which is much faster than the transition to the low energy state in the low-temperature reservoir. And due to the large diffusion coefficient, a particle stays in each box for the same amount of time, so the reaction in the fast-reaction box contributes more to the overall distribution and makes the high energy state more populated than the equilibrium state of average temperature.

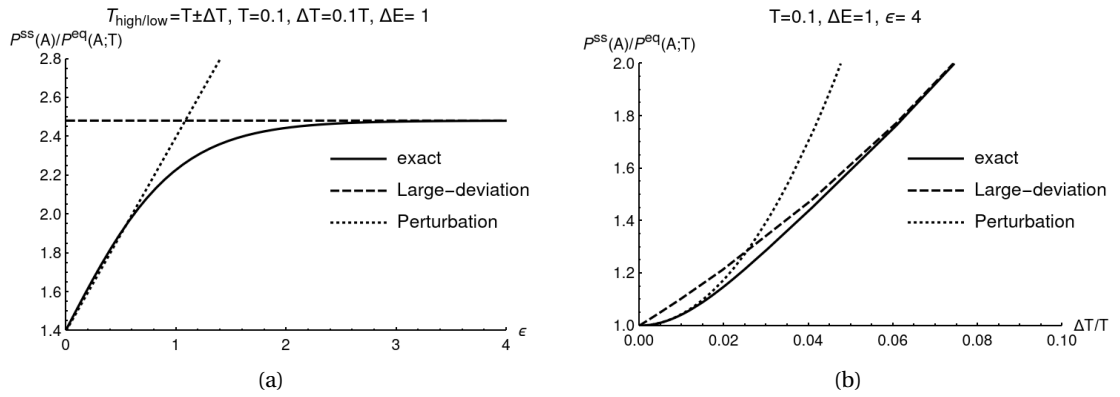


Figure 3.2 – a. The NESS-triggered kinetic stabilizing effect for varying energy barriers varies with the energy barrier. b. The NESS stabilizing varies with temperature difference. .

Now let us go to a more quantitative description of the stabilization effect. From Fig 3.2, the NESS solution shows two regimes. Indeed, these two regimes are predicted by Eq 3.13, i.e. the validity of perturbation theory. For a small temperature difference, the perturbation method is valid, and we can find a perturbation solution. In the large diffusion limit, we need to understand what exactly makes the system non-perturbative. Writing down the non-equilibrium transition rate from the high energy state to the low energy state, we see it can be approximated by two expressions for different cases:

$$\begin{aligned} \bar{k}_{BA} &= \frac{1}{2} \left(e^{-\epsilon/(T-\Delta T)} + e^{-\epsilon/(T+\Delta T)} \right) \simeq \frac{1}{2} e^{-\epsilon/T} \left(e^{\epsilon \Delta T/T^2} + e^{-\epsilon \Delta T/T^2} \right) \\ &\simeq \begin{cases} \frac{1}{2} e^{-\epsilon/(T+\Delta T)} & \epsilon \Delta T/T^2 \gg 1 \\ e^{-\epsilon/T} \left(1 + \frac{\epsilon^2 \Delta T^2}{2T^4} \right) & \epsilon \Delta T/T^2 \ll 1. \end{cases} \end{aligned} \quad (3.18)$$

The two regimes are determined by comparing the exponent $\epsilon \Delta T/T^2$ with 1. Using this criterion, we can separate the parameters space into a perturbative regime and a large-deviation regime and find the corresponding result, respectively.

Perturbative regime ($\epsilon \Delta T / T^2 \ll 1$): When the exponent $\epsilon \Delta / T^2$ is much smaller than one, we can do Taylor expansion and find a non-equilibrium transition rate as the equilibrium transition rate of T plus a second-order perturbative term. This is the so-called near-equilibrium condition, where the perturbation theory is valid and gives

$$\frac{P^{ss}(A)}{P^{eq}(A; T)} = 1 + P^{eq}(B; T) \frac{\Delta E(\Delta E - 2\epsilon)}{2T^4} \Delta T^2 + \mathcal{O}(\Delta T^3). \quad (3.19)$$

Large-deviation regime ($\epsilon \Delta T / T^2 \gg 1$): When the exponent $\epsilon \Delta / T^2$ is much greater than one, the transition rates in the high-temperature box are much faster than the rates in the low-temperature box, so the particles in the hot box reach an equilibrium distribution and then mediate by the fast diffusivity to maintain the particles in the cold box in the same distribution. Eventually, the steady-state probability distribution is equal to the equilibrium distribution of $T = T + \Delta T$, such that $P^{ss}(A) = P^{eq}(A; T + \Delta T)$. We can also name this regime the high-temperature regime since the probability distribution is fully dominated by the reactions under high temperatures.

3.4.2 Entropy production rate

We can further discuss how to understand this stabilization effect in terms of entropy production. In such a two-box system under NESS, the entropy production comes from the heat exchange with the two reservoirs:

$$\begin{aligned} \dot{S} &= \sum_{i=1,2} (k_{B_i A_i} P^{ss}(A_i) - k_{A_i B_i} P^{ss}(B_i)) \ln \left[\frac{k_{B_i A_i} P^{ss}(A_i)}{k_{A_i B_i} P^{ss}(B_i)} \right] + \sum_{X=A,B} (d_X P^{ss}(X_1) - d_X P^{ss}(X_2)) \ln \left[\frac{d_X P^{ss}(X_1)}{d_X P^{ss}(X_2)} \right] \\ &= \sum_{i=1,2} (k_{B_i A_i} P^{ss}(A_i) - k_{A_i B_i} P^{ss}(B_i)) \ln \left[\frac{k_{B_i A_i}}{k_{A_i B_i}} \right] \\ &= \sum_{i=1,2} J_{A_i \rightarrow B_i} \frac{\Delta E}{T_i} \\ &= \frac{Q}{T - \Delta T} - \frac{Q}{T + \Delta T} \\ &\approx \frac{2Q\Delta T}{T^2} > 0 \end{aligned} \quad (3.20)$$

The first equality comes from the entropy production rate of the master equation proposed by Schnakenberg[24]. In the large diffusion limit, $P^{ss}(X_1) = P^{ss}(X_2)$, so the entropy production of diffusion is zero. And the summation also cancels the entropy change inside the chemical reaction system. Hence we obtain the second equality. Letting $J_{A_i \rightarrow B_i} = k_{B_i A_i} P^{ss}(A_i) - k_{A_i B_i} P^{ss}(B_i)$ to denote the total flux from state A to B and using the definition of Kramers transition rate to relate the reaction rates to the energy landscape. $J_{A_i \rightarrow B_i} \Delta E$ is the heat expelled to the

environment in box i , so we obtain the thermodynamic form of the entropy production rate. In the perturbative regime, the entropy production rate starts from the second order of ΔT as

$$\dot{S} = P^{eq}(A; T) e^{-\varepsilon/T} \frac{\Delta E^2}{T^4} \Delta T^2 + \mathcal{O}(\Delta T^3). \quad (3.21)$$

As the deviation from equilibrium distribution also starts from the second order, we can relate it to the entropy production rate as

$$\frac{P^{ss}(A)}{P^{eq}(A; T)} = 1 + \frac{\dot{S}}{\Delta E} \frac{\Delta E + 2\varepsilon}{2e^{-(\Delta E + \varepsilon)/T}}. \quad (3.22)$$

Physically speaking, the entropy production rate quantifies the rate of dissipating energy. Thus we can interpret the payoff of high-energy stabilization as the continuously increasing of entropy in the environment. As we know the Boltzmann distribution maximizes the entropy of a canonical ensemble, the NESS here thus should have lower entropy than the thermodynamic equilibrium case. So the stabilization in a high energy state can also be named as maintaining a low entropy state by dissipating energy.

3.5 Three-state system: dissipation-driven selection

In the last section, we showed that a two-state reaction system can stabilize itself in the high-energy state by dissipating energy in a temperature gradient. Then we would like to study a little bit more complex model, which is a three-state system, where the non-equilibrium condition can lead to unbalance population of two states with equal energy. We call this phenomenon dissipation-driven selection[14].

3.5.1 Selection in large-diffusion limit

The energy landscape of the three-state system is plotted in Fig. 3.3a. The two low-energy states B and C have equal energy, and the transition between them is intermediated by the high-energy state A . The asymmetry is introduced by the kinetic terms, that the energy barrier from A to C is lower than the barrier from A to B . In equilibrium conditions, the two low energy states have equal probabilities, only reflecting the energetic character of the system. Then we put the three-state reaction system in a temperature gradient. Still, without loss of generality, the temperature gradient is simplified as a two-box model coupled to different temperature reservoirs, the evolution equation of the two-box three-state reaction-diffusion

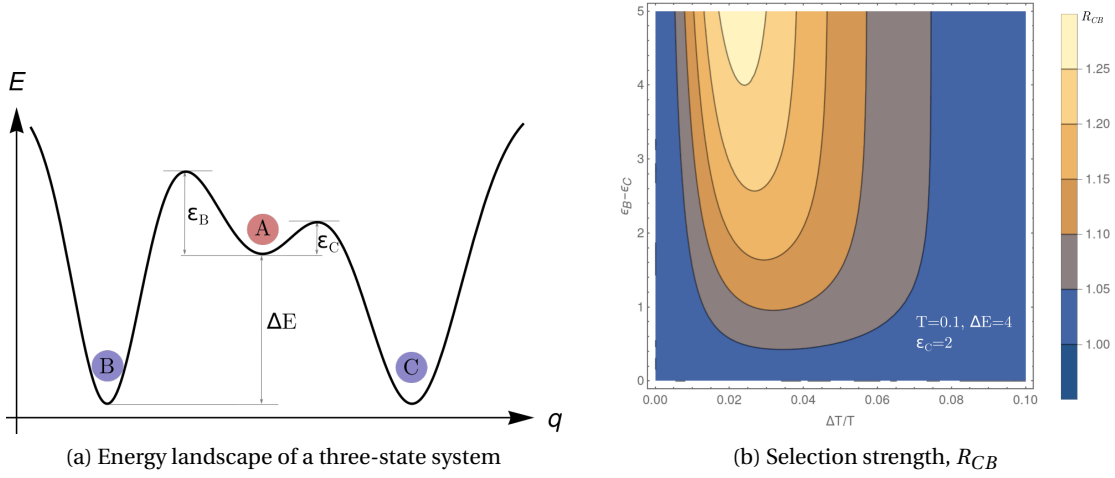


Figure 3.3 – a. The energy landscape of a three-state system. b. The selection strength $R_{CB} \equiv P^{ss}(C)/P^{ss}(B)$.

system is

$$\begin{aligned} \partial_t P(A_i) &= \sum_X (k_{A_i X_i} P(X_i) - k_{X_i A_i} P(A_i)) + d_A (P(A_j) - P(A_i)) \\ \partial_t P(X_i) &= k_{X_i A_i} P(A_i) - k_{A_i X_i} P(X_i) + d_X (P(X_j) - P(X_i)). \end{aligned} \quad (3.23)$$

where $X = B, C$, i , and j are indexes of the two boxes, d_x is the transport rate and the transition rates are of Kramers form. The energy of state A is ΔE higher than the energies of two low-energy states. The barriers from A to the two low energy states are ε_B and ε_C . Therefore the transition rate reads

$$k_{X_i A_i} = k_0 e^{-\varepsilon_X/T_i}, \quad k_{A_i X_i} = k_0 e^{-(\varepsilon_X + \Delta E)/T_i}, \quad (3.24)$$

where k_0 is a constant and the temperatures of the two boxes are $T_1 = T - \Delta T$ and $T_2 = T + \Delta T$. Still, we are interested in the large diffusion limit under which the above equations are reduced to Eq. 3.1 with non-equilibrium transition rates $\bar{k}_{XY} = (k_{X_1 Y_1} + k_{X_2 Y_2})/2$. The three states here is on a chain, so we know the NESS solution. To quantify the unbalance between the two low energy states, we can define a quantity called selection strength:

$$R_{CB} \equiv \frac{P^{ss}(C)}{P^{ss}(B)} = \frac{\bar{k}_{CA} \bar{k}_{AB}}{\bar{k}_{BA} \bar{k}_{AC}}. \quad (3.25)$$

When $\varepsilon_B > \varepsilon_C$, the selection strength R_{CB} is positive, i.e. the state with a lower energy barrier is favored. Then we would like to do some exploration of the parameters space to see how

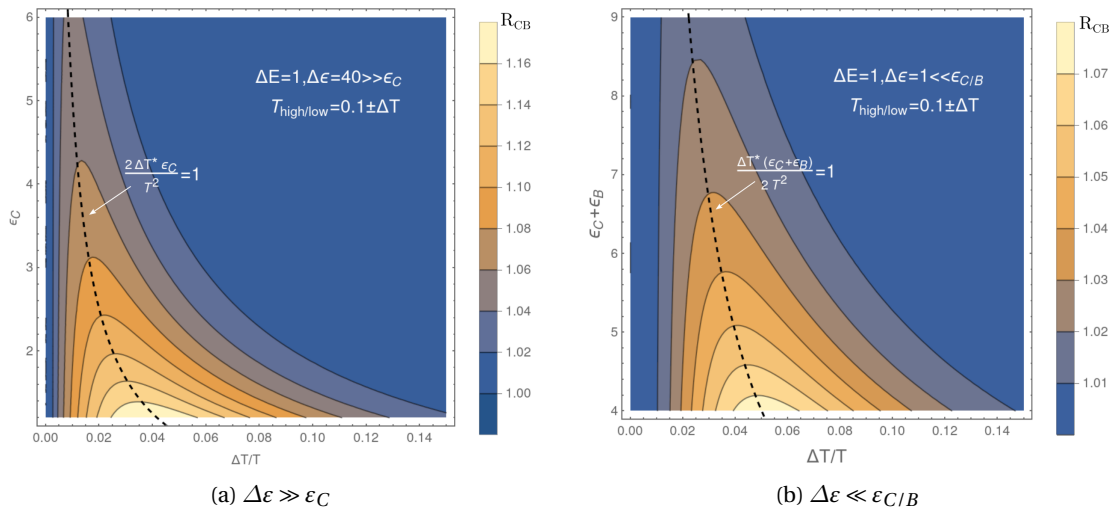


Figure 3.4 – Contour plots of the selection strength, R_{CB} , for small energy difference and large energy difference.

they change the selection strength. From Fig. 3.3b, we can observe that when keeping the barrier energy difference constant, the selection strength initially increases with temperature difference and then decreases back to 1. So there is an optimal temperature difference that maximizes the selection.

3.5.2 Optimal temperature for selection of three-state system

For small temperature differences, the can be obtained by the perturbation method. And in the last section, we see that in the non-perturbative regime, the chemical reaction is dominated by the reactions in the high-temperature box so that the system evolves to an equilibrium state corresponding to the Boltzmann distribution of the high temperature, and the unbalance vanishes. So an optimal temperature that maximizes the selection strength exists between the perturbative regime and large-deviation regime. By numerical exploration, we find that there are two cases for which we can give well approximated expressions for optimal temperature. One is for large barrier difference $\Delta\epsilon = \epsilon_B - \epsilon_C \gg \epsilon_C$ and the other is for small barrier difference $\Delta\epsilon \ll \epsilon_{B/C}$.

Optimal temperature when $\Delta\epsilon \gg \epsilon_C$

When the barrier difference is large enough, the slow reaction, the reaction between state B and A , is always operating in the large-deviation regime. Therefore the ratio between the NESS probabilities of B and A is $P^{ss}(B)/P^{ss}(A) = \exp(\Delta E/(T + \Delta T))$, which does not contain the kinetic parameters of the reaction, $\Delta T \epsilon_B / T^2 \gg 1$. So now we need to focus on the slow reaction. Supposing the reaction between state A and C is still operating in the perturbative

regime, we can find R_{CB} in the first two orders of ΔT as

$$\lim_{\frac{\Delta \varepsilon}{\varepsilon_C} \rightarrow +\infty} R_{CB} = 1 + \frac{\Delta E \Delta T}{T^2} - \frac{\Delta E \varepsilon_C \Delta T^2}{T^4} + \mathcal{O}(4\Delta T^3).$$

A local maximum is predicted by this expression, which is $\Delta T^* = T^2/(2\varepsilon_C)$. To check the correctness of this maximum, see Fig. 3.4a, where it predicts quite well.

Optimal temperature when $\Delta \varepsilon \ll \varepsilon_{C/B}$

When the barrier difference is small, both the fast and slow reaction operates in the same regime. Hence we can not just simply fix one and study the other. Then, let us first inspect the two solved regimes.

Perturbative regime When both $A \rightleftharpoons B$ and $A \rightleftharpoons C$ are operating in the perturbative regime, i.e. $\Delta T \varepsilon_{B/C}/T^2 \ll 1$ we can expand the selection strength in power of ΔT as

$$R_{CB} = 1 + \frac{\Delta E(\varepsilon_B - \varepsilon_C)\Delta T^2}{T^4} + \mathcal{O}(\Delta T^4). \quad (3.26)$$

In this scenario, the selection strength increases quadratically with ΔT . Apparently, R_{CB} cannot go to infinity. Thus we need to discuss the large-deviation case.

High-temperature regime In the high-temperature regime or the so-called large deviation-regime, as we discussed in Sec 3.4, the transition rate in the high-temperature box is significantly faster than in the cold box. We can thus expand the NESS probably distribution from the Boltzmann distribution of $T = T_{high}$ by treating the reaction in the cold box as a perturbation. The consequence selection strength is given by

$$R_{CB} = 1 + e^{-\varepsilon_C \Delta T/T^2} - e^{-\varepsilon_B \Delta T/T^2}. \quad (3.27)$$

With increasing of ΔT , the selection strength asymptotically relaxes to 1.

These two solutions suggest that the optimal temperature should appear between these two regimes. Thus it can be estimated by comparing $\Delta T(\varepsilon_B + \varepsilon_C)/(2T^2)$ with 1. We can guess the optimal temperature $\Delta T^* \simeq 2T^2/(\varepsilon_C + \varepsilon_B)$. As plotted in Fig. 3.5b and Fig. 3.4b, it's a good guess.

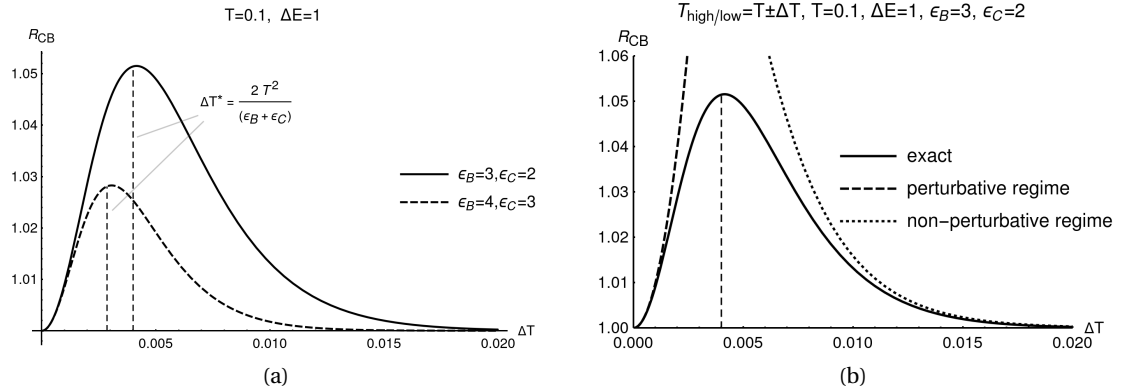


Figure 3.5 – a. Unbalance between $P(C)$ and $P(B)$ as a function of temperature difference. The three-state reaction system is coupled to two thermal reservoirs with temperature $T_1 = T - \Delta T$ and $T_2 = T + \Delta T$. The unbalancing is maximized around $\Delta T^* = 2T^2 / (\epsilon_C + \epsilon_B)$, i.e. the middle between the perturbative regime and non-perturbative regime. b. The perturbative regime and non-perturbative regime. For a small temperature difference, called the perturbative regime, the selection strength grows quadratically with ΔT . In the non-perturbative regime (but still $\Delta T/T \ll 1$), the high-temperature transition rates dominate and abolish the selection when ΔT gets larger.

3.5.3 Entropy production

As we mentioned in the title of this section, the temperature gradient-induced selection can be interpreted as the dissipation-driven selection. The physical quantity characterizing dissipation is the entropy production rate. Let us focus on the pure perturbative regime, and the selection strength is given by Eq. 3.26. The entropy production is

$$\dot{S} = \sum_{i=1,2} \sum_{X=B,C} J_{A_i \rightarrow X_i} \frac{\Delta E}{T_i} = P^{eq}(A; T) (e^{-\epsilon_C/T} + e^{-\epsilon_B/T}) \frac{\Delta E^2 \Delta T^2}{T^4}. \quad (3.28)$$

Now we can relate the selection strength to the entropy production rates as

$$R_{CB} = 1 + \frac{\dot{S}}{\Delta E} \frac{1}{P^{eq}(A; T) e^{-\epsilon_B/T}} \frac{\Delta \epsilon}{1 + e^{\Delta \epsilon/T}}. \quad (3.29)$$

This result tells us that selection strength is positively correlated to the entropy production rate. The entropy production in the environment can also be understood as a negative entropy flow to the reaction system so that the reaction system feeds on negative entropy to be able to distinguish two equal energy states. The ability to identify the internal kinetic structure is a form of information. By dissipating energy, the reaction system reaches a more organized state than an equally populated equilibrium state.

3.6 Autocatalysis

3.6.1 The mechanism of autocatalysis

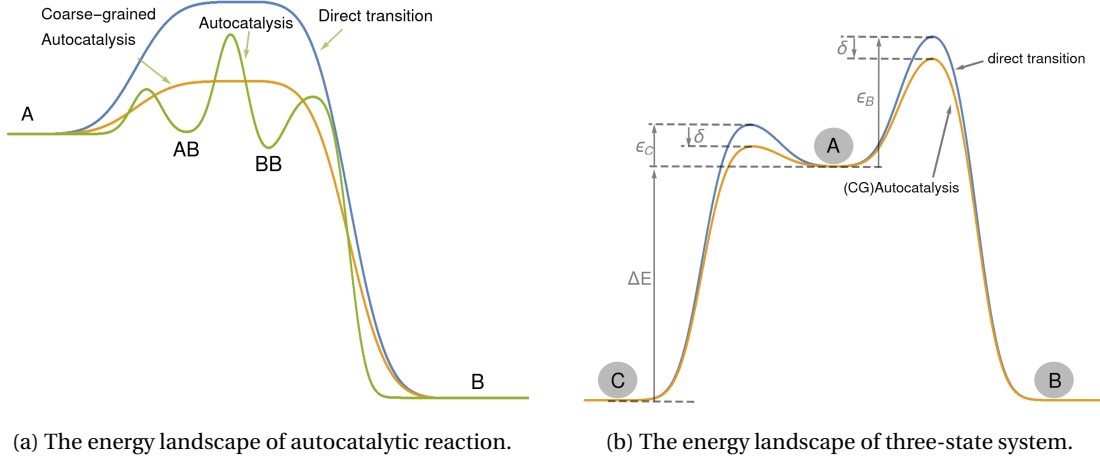


Figure 3.6 – a. The energy transition state AA and AB can be eliminated to find the coarse-grained autocatalysis energy landscape. b. The energy barriers of both sides are lowered by an amount of δ in an autocatalytic reaction.

A reaction called autocatalytic is when the product can catalyze its own reaction. The basic mechanism of autocatalytic particle B can bind with the substrate to lower the energy of the intermediate state AB , and then goes to BB and finally unbinding to release the product B , as shown in Fig. 3.6b. The overall chemical reaction can be written as



where AB and BB are the intermediate states. In seek of simplicity, we can coarse-grain the transition state by counting their effect as a lowering of the energy barrier by an amount of δ . The coarse-grained energy surface is shown in Fig. 3.6a. The reaction equation is non-linear

$$\begin{aligned} \frac{d}{dt}P(A) &= +f_{AB}^{cat}(P(B), P(A)) \\ \frac{d}{dt}P(B) &= -f_{AB}^{cat}(P(B), P(A)) \quad \text{where } f_{AB}^{cat}(P(B), P(A)) = -k_{BA}^{cat}P(A)P(B) + k_{AB}^{cat}P(B)^2. \end{aligned} \quad (3.31)$$

Under the coarse-grained scenario, only two new parameters is introduced: the lowered energy δ and a concentration-dependent parameter α . Hence the autocatalytic rate reads

$$k_{BA}^{cat} = \alpha e^{\beta\delta} k_{BA}, \quad k_{AB}^{cat} = \alpha e^{\beta\delta} k_{AB}, \quad (3.32)$$

where α is the other new parameter, which is a constant characterizing the magnitude of the transition rate, we can immediately see that the reaction rate is nothing but the direction-transition rate multiplying a temperature-dependent prefactor.

3.6.2 Three-state selection with autocatalysis

Now we can add a new species C to the autocatalytic reaction system as we did in the direct-transition reaction system, and make the energy barrier from A to C lower than that from A to B to induce the kinetic-symmetry breaking.

$$k_{CA}^{cat} = \alpha e^{\beta\delta} k_{CA}, \quad k_{AC}^{cat} = \alpha e^{\beta\delta} k_{AC} \quad \text{where } k_{CA} = k_0 e^{-\beta\epsilon_C} > k_0 e^{-\beta\epsilon_B}. \quad (3.33)$$

Placing the system in two connected boxes with different temperatures so that the system is in non-equilibrium condition. The corresponding reaction-diffusion equation is

$$\begin{aligned} \partial_t P(A_i) &= \sum_X P(X_i) \left(k_{A_i X_i}^{cat} P(X_i) - k_{X_i A_i}^{cat} P(A_i) \right) + d_A (P(A_j) - P(A_i)) \\ \partial_t P(X_i) &= P(X_i) (k_{X_i A_i}^{cat} P(A_i) - k_{A_i X_i}^{cat} P(X_i)) + d_X (P(X_j) - P(X_i)), \end{aligned} \quad (3.34)$$

where $X = B, C$ and the subscript i denotes the index of the box. The time evolution of the system can be obtained numerically. And we can also from the numerical result to obtain the NESS. We use the ratio of the probability of species B to species C to characterize the strength of selection. Starting from the initial state $P(B)^{(1)} = P(C)^{(1)} = P(B)^{(2)} = P(C)^{(2)} = 0.25$ and letting the system relax to steady-state for different external conditions, we can get the result as shown in Fig. 3.7.

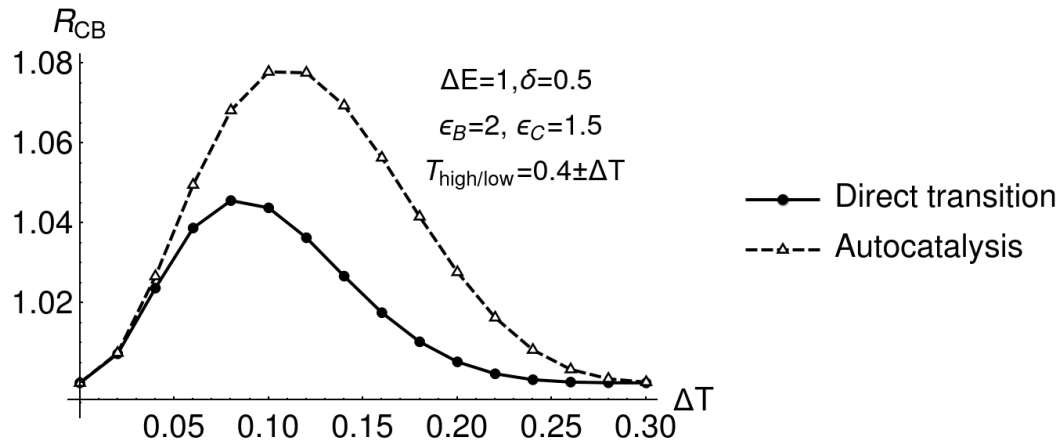


Figure 3.7 – A comparison of selection strength of direct-transition reaction and autocatalytic reaction.

We can see that autocatalysis also shows an optimal temperature for selection and always

shows to stronger selection than the direct-transition reaction. Note that we used very large diffusion coefficients which means we can use an infinite diffusion limit to obtain the analytic solution.

3.6.3 Analytic solution in the large diffusion regime

In the large diffusion limit, the probability of the same species in two boxes is equal $P(X_1) = P(X_2) = \frac{1}{2}P(X)$. One can sum up two equations of the same species in two boxes to obtain the effective reaction equation

$$\begin{aligned}\frac{d}{dt}P(A) &= \frac{1}{2} \left(\overline{k_{AB}^{cat}} P(B)^2 - \overline{k_{BA}^{cat}} P(A)P(B) + \overline{k_{AC}^{cat}} P(C)^2 - \overline{k_{AC}^{cat}} P(A)P(C) \right) \\ \frac{d}{dt}P(B) &= \frac{1}{2} \left(-\overline{k_{AB}^{cat}} P(B)^2 + \overline{k_{BA}^{cat}} P(A)P(B) \right) \\ \frac{d}{dt}P(C) &= \frac{1}{2} \left(-\overline{k_{AC}^{cat}} P(C)^2 + \overline{k_{AC}^{cat}} P(A)P(C) \right),\end{aligned}\quad (3.35)$$

where the effective reaction rate is the average of the rates in two boxes. The fixed point of this equation is determined by the linear part:

$$R_{CB}^{cat}(\varepsilon_B, \varepsilon_C, \delta) = \frac{P(C)}{P(B)} = \frac{\overline{k_{BA}^{cat}} \overline{k_{AC}^{cat}}}{\overline{k_{AB}^{cat}} \overline{k_{CA}^{cat}}}. \quad (3.36)$$

Writing it in an explicit form

$$\begin{aligned}R_{CB}^{cat} &= \frac{(e^{-\beta_1(\varepsilon_B - \delta)} + e^{-\beta_2(\varepsilon_B - \delta)})(e^{-\beta_1(\Delta E + \varepsilon_C - \delta)} + e^{-\beta_1(\Delta E + \varepsilon_C - \delta)})}{(e^{-\beta_1(\varepsilon_C - \delta)} + e^{-\beta_2(\varepsilon_C - \delta)})(e^{-\beta_1(\Delta E + \varepsilon_C - \delta)} + e^{-\beta_1(\Delta E + \varepsilon_C - \delta)})} \\ &= 1 + \frac{(e^{-\beta_1 \varepsilon_C} e^{-\beta_2 \varepsilon_B} - e^{-\beta_1 \varepsilon_B} e^{-\beta_2 \varepsilon_C})(e^{-\beta_1 \Delta E} - e^{-\beta_2 \Delta E})}{\frac{\sum_i e^{-\beta_i(\Delta E + \varepsilon_C + \varepsilon_B - 2\delta)}}{\sum_i e^{\beta_i \delta}} + (e^{-\beta_2 \varepsilon_C} e^{-\beta_1(\Delta E + \varepsilon_B)} + e^{-\beta_1 \varepsilon_C} e^{-\beta_2(\Delta E + \varepsilon_B)})} \\ &= 1 + \frac{g_1(\Delta E, \varepsilon_C, \varepsilon_B; \beta_1, \beta_2)}{g_2(\Delta E, \varepsilon_C, \varepsilon_B, \delta; \beta_1, \beta_2) + g_3(\Delta E, \varepsilon_C, \varepsilon_B; \beta_1, \beta_2)}.\end{aligned}\quad (3.37)$$

We can see that $g_1, g_2, g_3 > 0$, which means $R_{CB} > 1$, i.e. state C is favored. Note that only g_3 contains the contribution of autocatalysis, δ . And recall that for the direct transition, this ratio reads

$$R_{CB} = 1 + \frac{g_1}{g_2(\delta = 0) + g_3}. \quad (3.38)$$

They are differed only by the δ in g_2 . And we can then show the inequality:

$$g_2(\delta) = \frac{\sum_i e^{-\beta_i(\Delta E + \epsilon_C + \epsilon_B - 2\delta)}}{\sum_i e^{\beta_i \delta}} < \frac{\sum_i e^{-\beta_i(\Delta E + \epsilon_C + \epsilon_B)}}{2} = g_2(\delta = 0), \quad (3.39)$$

that means $R_{CB}^{cat} > R_{CB}$, i.e. the autocatalysis can boost selection in the large diffusion limit.

Indeed, this result is just a trivial extension of the selection of direct transition. In the large diffusion limit, the non-linear term does not change the fixed point. What changed the strength of selection is just the lowered energy barrier. We can construct a direct-transition reaction with energy $\epsilon_X = \epsilon_X - \delta$ to reach the same steady state as the autocatalytic reaction

$$R_{CB}^{cat} = R_{CB}(\epsilon_B \rightarrow \epsilon_B - \delta, \epsilon_C \rightarrow \epsilon_C - \delta), \quad (3.40)$$

3.6.4 Small diffusion - autocatalysis can either boost or suppress the selection

Boosting selection with $\delta = 0$

In previous discussions, we saw that the effect of autocatalysis is directly from the lowering of two energy barriers. If the autocatalytic prefactor does not depend on temperature (i.e. $\delta = 0$), the autocatalysis will give the same result as what the direct transition gives. However, when diffusion is small, $P(X_1) \neq P(X_2)$, gives the temperature-dependent non-linear effect. Thus autocatalysis can modulate the strength of selection again.

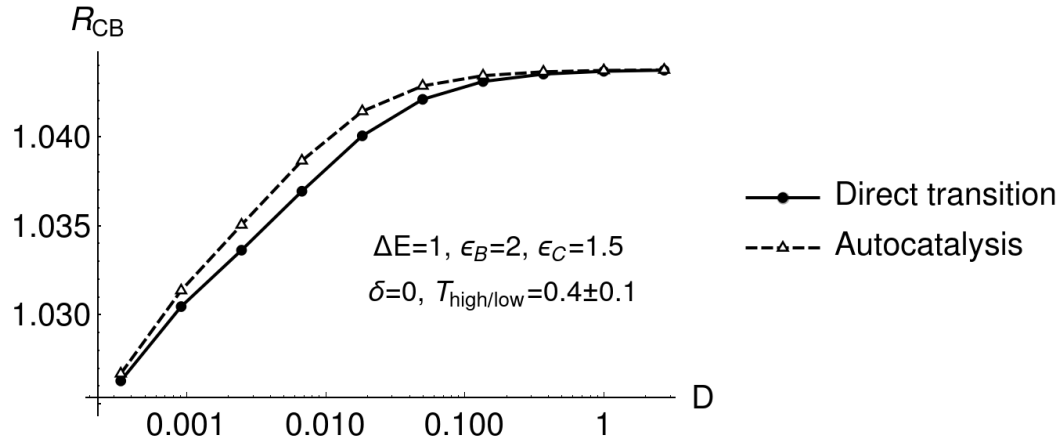


Figure 3.8 – Autocatalysis can boost selection even when it does not change the kinetic barriers.

From Fig. 3.8, we can see that the selection strength is larger with the non-linear term in comparison to the direct transition case. And as expected, it asymptotically approaches to direction transition case as D increases.

Suppressing selection for slow diffusion

Another interesting observation is that when the reaction is faster than diffusion ($\alpha, k_0 \gg D$), autocatalysis can suppress the selection. As shown in Fig. 3.9, R_{CB} of the autocatalytic reaction is smaller than that of direction transition for a small diffusion coefficient. And for the large diffusion coefficient, it enhances selection as predicted by Eq. 3.40.

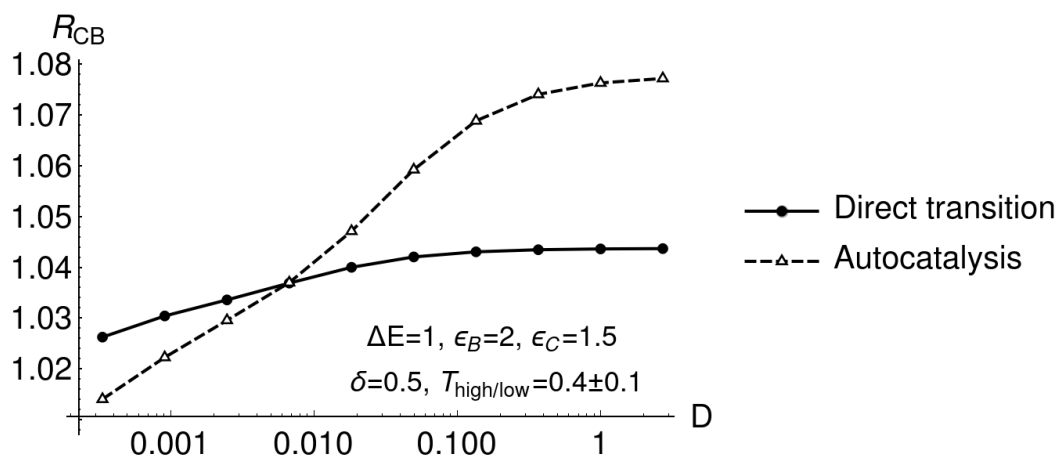


Figure 3.9 – Autocatalysis can suppress selection when the diffusion coefficient is very small.

4 Time-periodic temperature driving non-equilibrium chemical reactions

We have studied a reaction system brought out of equilibrium by a temperature gradient. The diffusion-reaction system maintained in a non-equilibrium steady state (NESS) shows bias to reactions with higher energy-dissipating rates. NESS is not only out of equilibrium state, but a periodic variation of external parameters can also mimic a NESS for both continuous and discrete system[25, 26]. The external parameters can be a periodically-varying temperature or chemical potential. This type of model are usually referred to as stochastic pumps(SP)[15, 27, 28]. Unlike most papers that discussed a time-periodic variation of energies and kinetic barriers, here we need to we introduce a periodic variation of (inverse-)temperature to mimic a temperature gradient-driven NESS.

4.1 Master equation with time-dependent transition rates

The master equation for an n-state reaction system of time-dependent transition rates reads

$$\partial_t p_i(t) = \sum_{j \neq i} (k_{ij}(t) p_j(t) - k_{ji}(t) p_i(t)). \quad (4.1)$$

For a thermodynamic system, the transition rates are of Kramers form

$$k_{ij}(t) \equiv k_{j \rightarrow i}(t) = k_0 \exp[-\beta(t) \mathcal{E}_{ij}], \quad (4.2)$$

where $\mathcal{E}_{ij} = \varepsilon + \max\{E_i - E_j, 0\}$ is the activation energy for the transition from state j to i , and k_0 is the rate constant. The thermodynamic parameter of the reservoir varies in time and leads to the transition rates being time-dependent.

4.1.1 Near-equilibrium approximation

The near-equilibrium approximation means that the time-dependent part can be treated as a small perturbation to a fixed temperature $T(t) = T_0 + \delta T_1(t)$. The time-dependent part is a periodic function with zero mean and period of τ . Let us suppose the time-dependent part of the form $T_1(t) = \tilde{T}_1 \sqrt{2} \sin \omega t$. Hence the average temperature is $\overline{T(t)} = T_0$ and the variance of the temperature is $\text{Var}(T) = \delta^2 \tilde{T}_1^2$. Since the perturbation is small, the inverse temperature can be expressed in a perturbative form:

$$\beta(t) = \beta_0 + \delta \beta_1(t) \quad \text{where } \delta \ll 1, \quad (4.3)$$

where $\beta_1(t) = \tilde{T}_1(t)/T_0^2$. For convenience, we use the inverse temperature in the following discussion. The transition rate can be expanded in powers of the perturbative (inverse-) temperature as

$$k_{ij}(t) = \sum_{n=0}^{\infty} \delta^n k_{ij}^{(n)} = \sum_{n=0}^{\infty} \frac{1}{n!} \delta^n (-\beta_1(t) \mathcal{E}_{ij})^n k_{ij}^{(0)}. \quad (4.4)$$

The n -th order term is $k_{ij}^{(n)} = \frac{1}{n!} (-\beta_1(t) \mathcal{E}_{ij})^n k_{ij}^{(0)}$. The probability distribution is also perturbed by the equilibrium distribution. So we do the same expansion for the probability distribution and find

$$p_i(t) = p_i^{(0)}(t) + \delta p_i^{(1)}(t) + \delta^2 p_i^{(2)}(t) + \mathcal{O}(\delta^3). \quad (4.5)$$

Substituting these two expansions into the master equation and collecting all terms of the same order of δ , we obtain

$$\begin{aligned} \text{0th order: } \quad \partial_t p_i^{(0)} &= \sum_{j \neq i} \left(k_{ij}^{(0)} p_j^{(0)} - k_{ji}^{(0)} p_i^{(0)} \right) \\ \text{1st order: } \quad \partial_t p_i^{(1)} &= \sum_{j \neq i} \left(k_{ij}^{(0)} p_j^{(1)} - k_{ji}^{(0)} p_i^{(1)} + k_{ij}^{(1)} p_j^{(0)} - k_{ji}^{(1)} p_i^{(0)} \right) \\ \text{2nd order: } \quad \partial_t p_i^{(2)} &= \sum_{j \neq i} \left(k_{ij}^{(0)} p_j^{(2)} - k_{ji}^{(0)} p_i^{(2)} + k_{ij}^{(1)} p_j^{(1)} - k_{ji}^{(1)} p_i^{(1)} + k_{ij}^{(2)} p_j^{(0)} - k_{ji}^{(2)} p_i^{(0)} \right). \end{aligned} \quad (4.6)$$

4.1.2 Zeroth-order and First-order solution

The zeroth-order equation describes a system in contact with a fixed-temperature heat bath. Such a system will relax to an equilibrium state which obeys detailed balance condition $p_i^{(0)} / p_j^{(0)} = k_{ij}^{(0)} / k_{ji}^{(0)} = e^{-\beta(E_i - E_j)}$. The detailed balance ensures the net flux between any two states is zero, i.e. the flux in the opposite direction is equal and cancels each other. Therefore we can denote the flux from state j to i as $J_{ij}^{(0)} = k_{ij}^{(0)} p_j^{(0)}$, which equals to $J_{ji}^{(0)} = k_{ji}^{(0)} p_i^{(0)}$.

Substituting the equilibrium solution of the zeroth-order into the first-order equation gives

$$\begin{aligned}
\partial_t p_i^{(1)} &= \sum_{j \neq i} \left(k_{ij}^{(0)} p_j^{(1)} - k_{ji}^{(0)} p_i^{(1)} - \beta_1(t) \mathcal{E}_{ij} J_{ij}^{(0)} + \beta_1(t) \mathcal{E}_{ji} J_{ji}^{(0)} \right) \\
&= \sum_{j \neq i} \left(k_{ij}^{(0)} p_j^{(1)} - k_{ji}^{(0)} p_i^{(1)} - \beta_1(t) (\mathcal{E}_{ij} - \mathcal{E}_{ji}) J_{ij}^{(0)} \right) \\
&= \sum_{j \neq i} \left(k_{ij}^{(0)} p_j^{(1)} - k_{ji}^{(0)} p_i^{(1)} - \beta_1(t) (E_i - E_j) J_{ij}^{(0)} \right).
\end{aligned} \tag{4.7}$$

Since the β_1 have zero mean over one period, we can take a one-period average of the above equation and find

$$0 = \sum_{j \neq i} \left(k_{ij}^{(0)} \overline{p_j^{(1)}} - k_{ji}^{(0)} \overline{p_i^{(1)}} \right). \tag{4.8}$$

The normalization condition requires $\sum_j p_j^{(1)}(t) = 0$, hence we find the one-period average of first-order probabilities are all zero, $\overline{p_i^{(1)}} = 0$. Then we need to focus on the second-order solution, where the non-equilibrium effect starts to appear. Before that, we need to calculate one more quantity that will appear in the second-order equation, that is $\overline{\beta_1 p_i^{(1)}}$. Multiplying $\beta(t)$ on both sides of Eq. 4.7 and averaging over one period, the RHS and LHS read

$$\begin{aligned}
LHS &= \frac{1}{\tau} \int_0^\tau \beta_1 \partial_t p_i^{(1)} dt \\
&= \frac{1}{\tau} \omega \int_0^\tau \tilde{P}_i^{(1)} \tilde{\beta}_i \cos(\omega t - \phi_i) \sin(\omega t) dt \quad \leftarrow p_i^{(1)} = \tilde{P}_i^{(1)} \sin(\omega t - \phi_i), \beta_1 = \tilde{\beta}_i \sin(\omega t) \\
&= \frac{\omega}{2} \tilde{P}_i^{(1)} \tilde{\beta}_i \sin \phi_i \\
&= \omega \overline{\beta_1 p_i^{(1)}} \tan \phi_i \\
RHS &= \sum_{j \neq i} \left(k_{ij}^{(0)} \overline{p_j^{(1)} \beta} - k_{ji}^{(0)} \overline{p_i^{(1)} \beta} - \overline{\beta_1^2} (E_i - E_j) J_{ij}^{(0)} \right).
\end{aligned} \tag{4.9}$$

The key assumption here is that the first-order solution has the form of $p_i^{(1)} = \tilde{P}_i^{(1)} \sin(\omega t - \phi_i)$, where ϕ_i is the phase delay with respect to the phase of temperature. This assumption is based on the dissipative nature of the reaction system, which does not have an intrinsic periodicity, so all its behaviors follow the externally driven term, here is the temperature. And it needs some time to respond to the externally driven term, so there should be a phase delay. The time scale of the LHS and RHS are characterized by ω and $k^{(0)}$ respectively, so we can compare them and find the solutions for the following two limits.

Fast-varying temperature

When the (inverse) temperature varies very fast, i.e. $\omega \gg k^{(0)}$, the LHS is much larger than the RHS, thus we get

$$\overline{\beta_1 p_j^{(1)}} \tan \phi_i = 0. \quad (4.10)$$

Intuitively speaking, $p_j^{(1)}$ can not catch up with the fast-varying temperature and thus the phase difference should not be zero. Therefore $\overline{\beta_1 p_j^{(1)}} = 0$.

Slowly-varying temperature

When the (inverse) temperature varies very slowly, i.e. $\omega \ll k^{(0)}$, the LHS is much smaller in comparison with RHS, so we can drop it and find

$$0 = \sum_{j \neq i} \left(k_{ij}^{(0)} \overline{p_j^{(1)}} \beta_1 - k_{ji}^{(0)} \overline{p_i^{(1)}} \beta_1 - \beta_1^2 (E_i - E_j) J_{ij}^{(0)} \right). \quad (4.11)$$

Then we can get the solution of $\overline{\beta_1 p_i}$ using generalized detailed balance condition

$$\frac{\overline{p_j^{(1)}} \beta_1 + \beta_1^2 E_j p_j^{(0)}}{\overline{p_i^{(1)}} \beta_1 + \beta_1^2 E_i p_i^{(0)}} = \frac{k_{ji}^{(0)}}{k_{ij}^{(0)}} = e^{-\beta_0 (E_j - E_i)}. \quad (4.12)$$

along with the normalization condition $\sum_i p_i^{(1)} = 0$, we get

$$\overline{p_i^{(1)}} \beta_1 = \beta_1^2 (\langle E \rangle - E_i) p_i^{(0)}. \quad (4.13)$$

4.1.3 Second order equation

Now we consider the fast-varying temperature case, under which $\overline{p^{(1)}(t) \beta_1(t)}$ are all zero. We can then substitute all the above results into the second-order equation and also integrate both sides over one period

$$0 = \sum_{j \neq i} \left(k_{ij}^{(0)} \overline{p_j^{(2)}} - k_{ji}^{(0)} \overline{p_i^{(2)}} + \frac{1}{2} \beta_1^2 (\mathcal{E}_{ij}^2 - \mathcal{E}_{ji}^2) J_{ij}^{(0)} \right). \quad (4.14)$$

Here the detailed balance condition is broken by an additional term $\frac{1}{2} \beta_1^2 (\mathcal{E}_{ij}^2 - \mathcal{E}_{ji}^2) J_{ij}^{(0)}$. Note that this term is induced by the perturbative temperature and also has a dependence on the kinetic barrier. So the second-order solution is not solely determined by energetic parameters but also by kinetic parameters of the reaction network. In the next section, we will use this

result to show selection due to different dissipation rates and non-equilibrium conditions in the three-state system.

4.2 Three-state system and the dissipation-driven selection

Let us consider the three-state reaction system proposed in Sec. 3.5 in a periodic-varying (inverse) temperature, $\beta(t) = \beta_0 + \delta\beta_1(t)$. In the perturbative regime, with the assumption of slowly-varying temperature, we can find the zeroth-order solution is the Boltzmann equilibrium distribution, and the first order is zero. Thus, the selection starts with the second order. Using the above result, we can directly write down the steady-state equation for the one-period-averaged second-order probability distribution of the three-states system

$$\begin{aligned} 0 &= k_{A \rightarrow X}^{(0)} \overline{p_A^{(2)}} - k_{X \rightarrow A}^{(0)} \overline{p_B^{(2)}} - \frac{\overline{\beta_1^2}}{2} (2\varepsilon_X \Delta E + \Delta E^2) J_{A \rightarrow X}^{(0)} \\ 0 &= \overline{p_A^{(2)}} + \overline{p_B^{(2)}} + \overline{p_C^{(2)}}, \end{aligned} \quad (4.15)$$

where ε_X is the kinetic barrier from state A to X and $X = B, C$ are the two low energy states. The last equation comes from the conservation of the total probability. For such a linear system, we can get the solution easily and calculate the selection strength

$$R_{CB} \equiv \frac{P(C)}{P(B)} \equiv \frac{\overline{p_C}}{\overline{p_B}} = 1 + \Delta E \overline{\beta_1^2} (\varepsilon_B - \varepsilon_C) \delta^2 + \mathcal{O}(\delta^4). \quad (4.16)$$

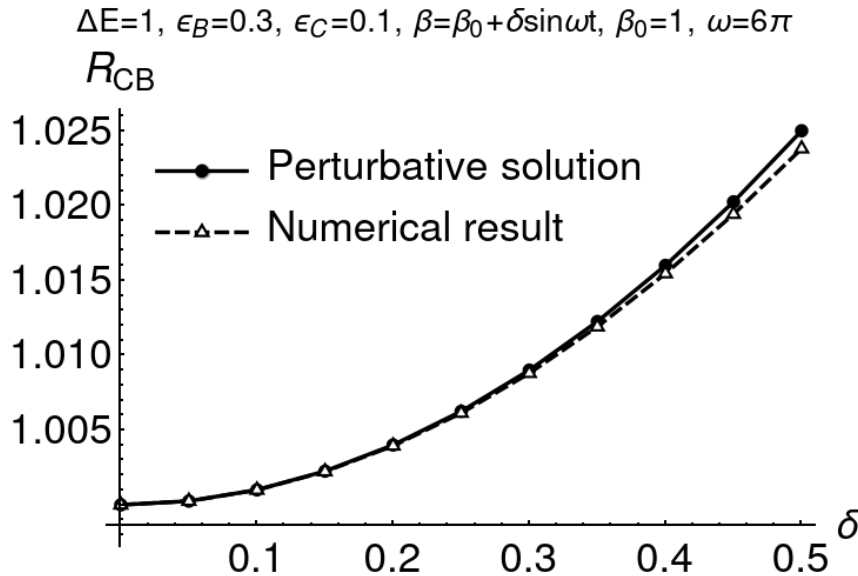


Figure 4.1 – Numerical and perturbative solution of selection strength of the three-state system in periodic temperature with parameters $\beta_0 = 1, \beta_1(t) = \sin \omega t, \omega = 2\pi, \Delta E = 1, \varepsilon_C = 0.3, \varepsilon_B = 0.1$.

This result is very similar to what we have obtained for the temperature gradient case. For the numerical simulation, the time-periodically-varying temperature is $\beta = \beta_0 + \delta \sin \omega t$. And we can see from Fig. 4.1 that the two results match quite well for small δ , as expected for the near-equilibrium approximation.

4.2.1 Entropy production

Using Schnakenberg's formula of entropy production rate, the entropy production rate over one period is

$$\begin{aligned}
 \bar{S} &= \frac{1}{2} \int_0^\tau dt \sum_i (\beta_0 + \delta \beta_1) \sum_{j \neq i} (k_{ij} p_j - k_{ji} p_i) \ln \left[\frac{k_{ij}}{k_{ji}} \right] \\
 &= -\frac{1}{2} \int_0^\tau \sum_i \sum_{j \neq i} (k_{ij} p_j - k_{ji} p_i) (\beta_0 + \delta \beta_1) \Delta E_{ij} \\
 &= \frac{1}{4} \delta^2 \int_0^\tau \sum_i \sum_{j \neq i} (k_{ij}^{(0)} p_j^{(0)} \mathcal{E}_{ij} - k_{ji}^{(0)} p_i^{(0)} \mathcal{E}_{ji}) \beta_1^2(t) \Delta E_{ij} \\
 &= \frac{1}{2} \delta^2 \bar{\beta}_1^2 \sum_i \sum_{j \neq i} J_{ij}^{(0)} \Delta E_{ij}^2.
 \end{aligned} \tag{4.17}$$

For the three-state system, it is written as

$$\begin{aligned}
 \bar{S} &= \delta^2 \bar{\beta}_1^2 \Delta E^2 p_A^{(0)} (k_{A \rightarrow C}^{(0)} + k_{A \rightarrow B}^{(0)}) \\
 &= \delta^2 \bar{\beta}_1^2 \Delta E^2 p_A^{(0)} e^{-\beta_0 \varepsilon_C} (1 + e^{-\beta_0 (\varepsilon_B - \varepsilon_C)}).
 \end{aligned} \tag{4.18}$$

Then we can relate it to the selection strength

$$R_{CB} = 1 + \frac{\bar{S}}{\Delta E} \frac{1}{P^{eq}(A, T_0) e^{-\beta_0 \varepsilon_B}} \frac{\Delta \varepsilon}{1 + e^{\beta_0 \Delta \varepsilon}}, \tag{4.19}$$

where $\Delta \varepsilon = \varepsilon_B - \varepsilon_C$. This expression is an analogy to Eq. 3.26 and indicates that the selection is also driven by dissipating energy.

4.3 Physical interpretations and applications

4.3.1 Chemical reactions in convection current

We have seen that time-periodically varying temperatures can maintain a system out of equilibrium and induce selection, but does such a system exist in nature? The answer is yes. Moreover, it might play a more important role in the origins of life in comparison to the reaction-diffusion mechanism in a temperature gradient. Imaging chemical reactions near hydrothermal vents on the seafloor, the temperature gradient is so sharp that the mass

transport is governed by convection instead of diffusion. Reacting chemicals carried by the convection current go and back between the hot and cold regions and feel a time-periodically changing temperature.

4.3.2 Reaction systems coupled to small reservoirs

A chemical reaction system with fixed rates is required to be coupled to an ideal infinite large heat reservoir so that the temperature fluctuation is negligible. However, in real life, the heat reservoir is finite, which means we must take account of the fluctuation of temperature, which can be written as an average temperature plus noise term

$$T = \langle T \rangle + \sqrt{\langle \Delta T^2 \rangle} \eta(t), \quad (4.20)$$

where $\eta(t)$ is a Gaussian white noise, $\langle \eta(t) \rangle = 0$, $\langle \eta(t)^2 \rangle = 1$. And the inverse temperature reads

$$\beta = \frac{1}{T} = \frac{1}{\langle T \rangle} + \frac{\sqrt{\langle \Delta T^2 \rangle}}{\langle T \rangle^2} \eta(t). \quad (4.21)$$

Comparing this expression with the time-periodic varying case, we see an analogy: $\beta_0 = 1/\langle T \rangle$ and $\delta\beta_1(t) = \sqrt{\langle \Delta T^2 \rangle}/\langle T \rangle^2 \eta(t)$. The only difference is that the time-periodically varying part is replaced by a noise term. However, we can still follow all steps of the previous derivation but replace the one-period integral with long time average and finally obtain very similar results

$$R_{CB} = 1 + \Delta E \frac{\langle \Delta T^2 \rangle}{\langle T \rangle^4} (\varepsilon_B - \varepsilon_C) + \mathcal{O}(\langle \Delta T^2 \rangle^2). \quad (4.22)$$

This result shows how chemical reaction systems respond to temperature fluctuation. And since it is a fluctuation, the near-equilibrium assumption is guaranteed by itself, so the perturbative solution is more suitable.

5 Thermophoresis

5.1 Introduction

In a dispersion system, the temperature gradient can trigger particles to migrate to a cold or hot region without a real external force. This effect is commonly called the Ludwig-Soret effect, thermophoresis, or thermodiffusion. These phenomena have been observed in various mixtures, such as colloidal suspension, bimolecular solution, and fluid mixture. Since its first discovery by Ludwig in 1856, a lot of experimental and theoretical work has been done, but a widely accepted theoretical explanation is still lacking [29–31]. The difficulty is that the main experimental features, such as the amplitude of the thermophoretic effect, are system-specific and the detailed microscopic nature of particle/solution interaction seems to be non-negligible [32]. Thermophoresis, as a typical non-equilibrium system is interesting by itself. Moreover, it is a promising tool to control microparticles in dispersion systems.

Thermophoresis is characterized by a drift flux, which is induced by the temperature gradient. This flux competes with the Brownian motion, i.e. the Fick's diffusion flux, to form a non-uniform concentration distribution. Therefore the total flux is

$$J = -D_T c \nabla T - D \nabla c. \quad (5.1)$$

where c is the concentration of particle, D_T is the thermodiffusion coefficient, D is the Fick's diffusion coefficient. The first thermophoretic term tends to build up a concentration gradient along the temperature gradient, while the second diffusive term tends to flatten the concentration distribution. The thermodiffusion coefficient is defined under a balance between these two terms, i.e. the steady state when total flux equals to zero.

$$D_T \equiv -\frac{D \nabla c}{c \nabla T}. \quad (5.2)$$

Another widely used parameter to quantify thermophoresis is $S_T = \frac{D_T}{D}$, namely the Soret coefficient. The Soret coefficient can be positive or negative, corresponding to the preference

of cold or hot regions for particles, respectively.

There exist two different types of models to explain thermophoretic phenomena, hydrodynamic and thermodynamic models [33]. The hydrodynamic picture considers the pressure difference caused by fluid thermo-osmotic flow around a particle [34] while the thermodynamic model constructs a thermodynamic gradient or excess enthalpy to describe the thermophoretic force.

We recently reported that multi-state particles show thermophoresis-like behavior [14]. And here we will give a complete picture of the multi-state contribution to thermophoresis. It is believed that the multi-state contribution should dominate the thermophoresis of small particles, as the small particles are too small to feel the temperature gradient directly.

In Sec 5.2, we address that the non-uniform concentration of particle dispersion can come from positional dependent diffusion coefficient. In Sec 5.3, we propose a multi-state particle model to show how can temperature gradient induces a positional-dependent diffusion coefficient. The multi-state model is then generalized to continuous chemical space cases. For particles without distinct states, such as spherical colloidal particles, we solve the Kramers equation using the time-scale separation approach to illustrate that the velocity can be regarded as an internal state and thus lead to thermophoresis. The contribution of particle-particle interaction is also included as a possible origin of the negative Soret coefficient.

5.2 Spatially dependent diffusion coefficient

Non-uniform distribution of particle suspension has been observed in various inhomogeneous system[35]. This kind of phenomenon can be described by the generalization of Fick's diffusive flux, that is the Fokker-Planck flux. Unlike Fick's flux, $J_{fick} = D\nabla c$, the Fokker-Planck flux put the diffusion coefficient inside the derivative, $J_{FP} = \nabla(D(x)c)$. So that a drift term comes out consequently

$$J_{FP} = - \underbrace{c\nabla D}_{\text{drift flux}} - \underbrace{D\nabla c}_{\text{diffusion flux}} . \quad (5.3)$$

The drift flux is nonzero if the diffusion coefficient depends on the position. Comparing this drift flux with the thermophoretic drift flux in Eq. (5.1), one can notice that the thermodiffusion coefficient emerges from the temperature-dependent diffusion coefficient, $D_T = \frac{\nabla D}{\nabla T} = \nabla_T D$. The role of temperature gradient in thermophoresis is to turn the temperature dependence of the diffusivity into positional dependence. This effect was pointed out in very early research on thermophoresis by Chapman in 1928 [36] and was recently discussed by Yang et al. [37, 38].

Under this scenario, the key point to understanding thermophoresis is to find the temperature dependence of the diffusion coefficient. Here we propose a multi-state particle model, where a state of a particle is associated with an energy and a diffusion coefficient, to show how the temperature affects the effective diffusivity of the particle.

5.3 Multiple-state particle in temperature gradient

5.3.1 Multi-state particle

The multi-state model captures the internal degrees of freedom of a particle. For example, a polymer chain is composed of many monomers, so the different configurations of a polymer chain can be regarded as a collection of states. According to the Einstein-Stokes relation, the diffusion coefficient depends on the size of the particle; thus, different configurations of the polymer chain can have different sizes, which leads to different diffusion coefficients. In 1967, T. N. Khazanovich [39] showed that one could integrate over the configuration space of a polymer chain to find thermophoresis behavior. This framework can be extended to a more general reaction-diffusion system, where the reaction characterizes the transition between states of the particle.

Discrete states

Let us start from a simple model, a particle with n discrete states $\{i\} = (1, 2, \dots, n)$. The chemical reaction here is isomerization reaction $X_i \leftrightarrow X_j$. The transitions among the discrete states are captured by a Markov jump process. Without loss of generality but with a lot of simplicity, we can restrict ourselves to one-dimensional space. Then the reaction-diffusion equation reads

$$\partial_t c_i = D_i \partial_x^2 c_i + \sum_{j=1}^n K_{ij} c_j, \quad (5.4)$$

The first term on the right-hand side captures the diffusion in space, where D_i is the diffusion coefficient of state i . For simplicity, we assume that the diffusion coefficient for a single state is constant in space. While the second term is the reaction part, where state i can spontaneously jump to state j with a rate of K_{ij} . In order to recover Boltzmann distribution in chemical space under the non-diffusion limit, the transition should be Arrhenius-like, i.e. $K_{ij} = K_{ji} e^{-\beta(E_j - E_i)}$.

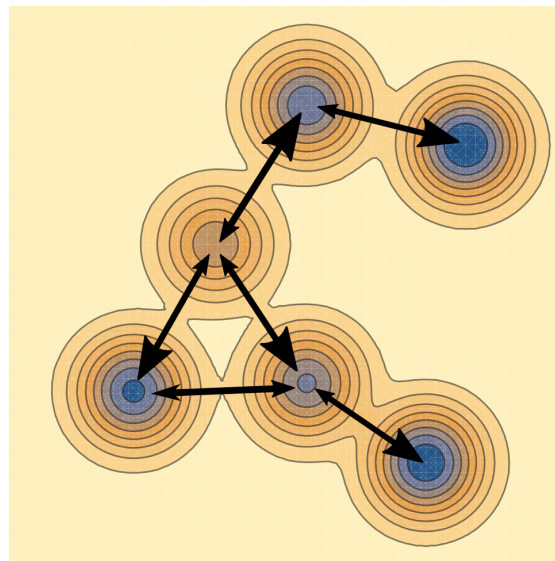
By summing over all states, the reaction terms cancel, as required by the conservation of probability.

$$\partial_t c_{tot} = \sum_i \partial_x^2 (D_i c_i) = \partial_x \left(\underbrace{\partial_x \sum_i D_i c_i}_{-J_{tot}} \right). \quad (5.5)$$

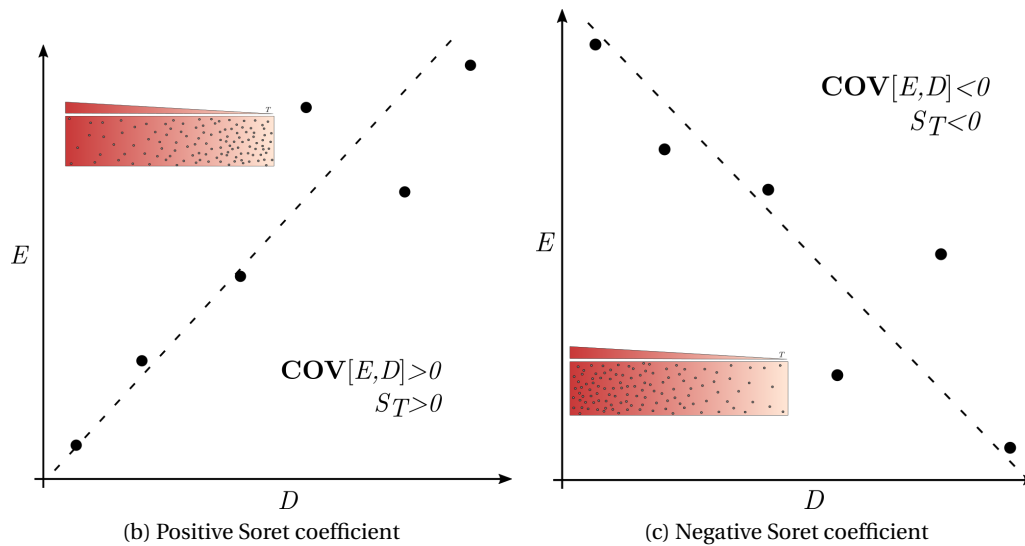
Note that the total flux can be written in a Fokker-Planck flux form by defining $D(x) \equiv \frac{\sum_i D_i c_i}{\sum_i c_i} = \langle D_i \rangle$. Consequently, the positional dependence of the diffusion coefficient emerges from the temperature-induced distribution in chemical space.

In the steady-state, i.e. $\partial_t c_{tot} = 0$. This position-dependent diffusion coefficient together with the non-flux boundary condition will induce the non-uniform distribution of particles, which is characterized by

$$0 = J_{tot} = -\langle D \rangle \partial_x c_{tot} - c_{tot} \partial_x \langle D \rangle \quad (5.6)$$



(a) Chemical reaction network



(b) Positive Soret coefficient

(c) Negative Soret coefficient

Figure 5.1 – a. Contour plot of the energy landscape of a six-state chemical reaction network, the local minimums (potential wells) can be regarded as discrete states. b. When the ensemble covariance of energies and diffusion coefficients of states are positive, the Soret coefficient is positive so that the particles accumulate on the cold side. c. For the negative covariance, the particle has a negative Soret coefficient and tend to stay on the hot side

In comparison with the definition of thermophoresis, the thermodiffusion coefficient, as well as the Soret coefficient comes out naturally:

$$D_T = \partial_T \langle D \rangle, \quad S_T \equiv \frac{D_T}{\langle D \rangle} = \frac{\partial_T \langle D \rangle}{\langle D \rangle}. \quad (5.7)$$

Supposing local equilibrium condition, i.e. the transition between states is much faster than the diffusion, the local state distribution follows Boltzmann equilibrium, $c_i \simeq c_{tot} e^{-\beta E_i} / Z$. Thus the effective diffusivity can be written in an exact form $D = \frac{1}{Z} \sum_i D_i e^{-\beta E_i}$. Then the corresponding Soret coefficient is

$$S_T = \frac{\langle ED \rangle - \langle E \rangle \langle D \rangle}{\langle D \rangle T^2} = \frac{\mathbf{Cov}(E, D)}{\langle D \rangle T^2}, \quad (5.8)$$

where $\langle \cdot \rangle = \frac{1}{Z} \sum_i \cdot e^{-\beta E_i}$. This expression provides physical insights into the thermophoresis problem from an energetic perspective. If the energy and diffusion coefficient are positively correlated, i.e. the high energy state particle diffuses faster, then the Soret coefficient is positive, and the particles tend to move from the hot region to the cold region and vice versa.

Continuous chemical space

The above result can be generalized to the continuous chemical space, which is expanded by the internal degrees of freedom of a molecule/particle. The reaction-diffusion equation, as a coarse-grained description of the transition among local minimums in the continuous chemical space (Fig ??), is not valid anymore. The Langevin equation, Newton's equation of motion with noise term, can capture both the chemical space and real space in a coherent manner. Let us suppose the viscosity is high enough so that the system is in the over-damped regime. The over-damped Langevin equation reads

$$\dot{x} = \sqrt{2D_x(x, q)} \eta(t). \quad (5.9)$$

The chemical space is expanded by internal degrees of freedom $\mathbf{q} = [q_1, \dots, q_n]$. And a given configuration of internal degrees of freedom is associated with energy $U(\mathbf{q})$. The equation of motion of the internal states is also characterized by a Langevin equation

$$\dot{\mathbf{q}} = -\frac{1}{\gamma_q} \nabla_q U_q(\mathbf{q}) + \sqrt{2D_q(\mathbf{q})} \eta_q(t), \quad (5.10)$$

where $U_q(\mathbf{q})$ is the chemical potential of a given configuration \mathbf{q} , $D_q(\mathbf{q})$ is the effective diffusion coefficient in chemical space and $\eta_q(t)$ is white noise. Then the corresponding Fokker-Planck

equation is

$$\partial_t P = \underbrace{\nabla_q \left(\frac{1}{\gamma_q} P \nabla_q U_q + \nabla_q (D_q P) \right)}_{-J_q} + \underbrace{\partial_x (\partial_x (D_x P))}_{-J_x}. \quad (5.11)$$

where $P \equiv P(x, q)$, is the probability distribution on the position-chemical space. Thermophoresis requires chemical-state-dependent diffusion coefficient, $D_x(q) \equiv a(q) \tilde{D}_x$, here the state-dependence is characterized by $a(q) \sim 1$ and a constant \tilde{D}_x denotes the amplitude. The fast reaction limit is of the most interest. For continuous chemical space, the fast reaction limit means the diffusion in the chemical space is much faster than the real space, $D_q \gg D_x$. Let $\delta \equiv \frac{\tilde{D}_x}{D_q}$, the time-independent (steady-state) F-P equation reads

$$a(q) \delta \partial_x P = -\partial_q^2 P - \frac{1}{k_B T(x)} \partial_q (P \partial_q U_q). \quad (5.12)$$

Then the probability density can be expanded in terms of δ :

$$P = P^{(0)} + \delta P^{(1)} + \delta^2 P^{(2)} + \mathcal{O}(\delta^3). \quad (5.13)$$

Substituting the expanded probability distribution back to the F-P equation and collecting terms with the same order of δ gives

$$\begin{aligned} 0 &= -\partial_q^2 P^{(0)} - \frac{1}{k_B T(x)} \partial_q (P^{(0)} \partial_q U_q) \\ a(q) \partial_x P^{(0)} &= -\partial_q^2 P^{(1)} - \frac{1}{k_B T(x)} \partial_q (P^{(1)} \partial_q U_q). \end{aligned} \quad (5.14)$$

The zeroth-order equation simply gives the Boltzmann distribution in chemical space multiplying an ungerminated function $\phi(x)$, which needs to be determined by the first-order equation.

$$P^{(0)}(x, q) = \phi(x) \exp\left(-\frac{U_q}{k_B T(x)}\right). \quad (5.15)$$

Note that the accessible chemical space is finite, hence there is no flux from $\lim_{q \rightarrow \pm\infty}$, we can integrate the above result over the whole chemical space to get the marginal distribution

$$\partial_x^2 \left(\underbrace{\phi(x) Z_q}_{\Phi(x)} \underbrace{\frac{1}{Z_q} \int_{-\infty}^{\infty} dq \phi(x) a(q) \exp\left(-\frac{U_q}{k_B T}\right)}_{D_{eff}/\tilde{D}_x} \right) = 0, \quad (5.16)$$

where $\Phi(x) = \int_d dq P_0(x, q)$ is the marginal distribution along x , the other term is the average of the D_x in q space. Writing the ensemble average in chemical space as $\langle \cdot \rangle_q = \frac{1}{Z_q} \int_q dq \cdot$

$\exp\left(-\frac{U_q}{k_B T}\right)$, we obtain

$$\partial_x^2(\Phi(x)\langle D_x \rangle_q) = 0, \quad (5.17)$$

which are the same as the discrete state case. The Soret coefficient can also be written as

$$S_T = \frac{\partial_T \langle D_x \rangle_q}{\langle D_x \rangle_q} = \frac{\mathbf{Cov}(E, D_x)}{\langle D_x \rangle_q}. \quad (5.18)$$

5.3.2 Particle with single chemical-state

In all the above derivations, we suppose the diffusion coefficient of each state does not depend on temperature. However, if we introduce the temperature dependence of single species diffusivity, the above derivation still holds. And we can even see thermophoresis for single-state particles. The basic temperature dependence of D is from the Stokes-Einstein relation, $D = \frac{k_B T}{\gamma}$, and the corresponding Soret coefficient is $S_T = \frac{1}{T}$. However, the validity of the Stokes-Einstein relation in the non-equilibrium state is under debate. In the scheme of the over-damped Langevin equation, this problem turns to the Ito-Stratonovich dilemma [37, 40], i.e. what is the proper stochastic integration convention for multiplicative noise. To avoid this problem, we can solve the Kramers equation instead. The Kramers equation is the Fokker-Planck equation of the under-damped Langevin equation, where the x -dependent multiplicative noise does not couple with the velocity. The Kramers equation reads

$$\partial_t P + v \partial_x P = \frac{\gamma}{m} \partial_v \left(v P + \frac{T(x)}{m} \partial_v P \right), \quad (5.19)$$

where $P \equiv P(x, v, t)$ is the probability distribution in the position-velocity space, γ is the friction, m is the mass of particle, $T(x)$ is the temperature, which depends on position. What we are interested in is the overdamped region, i.e. the friction dominates over the inertial term. The overdamped regime can be defined by a physical quantity with the scale of time $\tau = \frac{\gamma}{m} \ll 1$, the ratio of mass to friction provides a much faster time scale than all other physical processes, thus we can employ time-scale separation technics to solve for the marginal distribution (See supplementary material). Finally, we can reach a Smoluchowski equation

$$\partial_t \Phi(x, t) = \partial_x \left[\partial_x \left(\frac{\langle v^2 \rangle}{\langle 1 \rangle} \Phi(x, t) \right) \right], \quad (5.20)$$

where $\langle \cdot \rangle = \int_v \cdot e^{-\frac{v^2}{T(x)}} dv$, Φ is the marginal probability distribution in positional space. This equation is the standard Smoluchowski equation if we identify $D(x) = \frac{\langle v^2 \rangle}{\langle 1 \rangle} \propto T(x)$. Then the corresponding Soret coefficient is $S_T = \frac{1}{T}$.

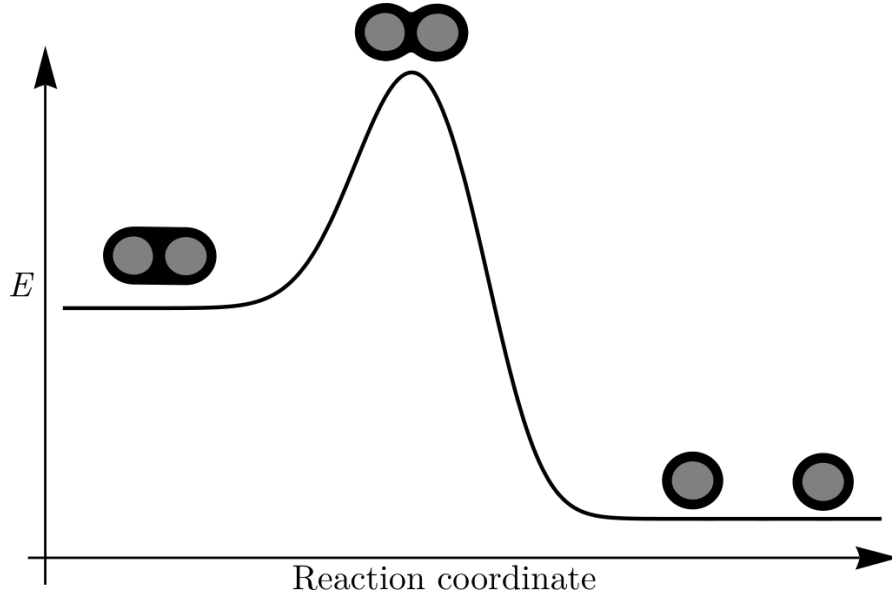


Figure 5.2 – The energy landscape of the binding and unbinding states. Dimers diffuse slower than monomers since the effective radius is larger.

5.3.3 Negative Soret coefficient due to particle-particle interaction

Now let us consider non-diluted colloid suspension, where the interaction between colloidal particles is not negligible. In such an environment, two-particle can bind to form a dimer, and the dimer still moves diffusely. The reaction-diffusion equation for such a model can be written as

$$\begin{aligned}\partial_t c_1 &= 2k_- c_2 - 2k_+ c_1^2 + D_1 \nabla c_1 \\ \partial_t c_2 &= k_+ c_1^2 - k_- c_2 + D_2 \nabla c_2,\end{aligned}\tag{5.21}$$

where c_1 and c_2 are the concentration of the monomers and dimers, respectively. With the mass conservation condition $c_1 + 2c_2 = c_{tot}$ and defining the association constant $K \equiv \frac{k_+}{k_-}$, the equilibrium solution of the chemical reaction part is

$$\begin{aligned}c_1^{(eq)}(K) &= \frac{\sqrt{1 + 8Kc_{tot}} - 1}{2K} \\ c_2^{(eq)}(K) &= \frac{4Kc_{tot} + 1 - \sqrt{1 + 8Kc_{tot}}}{4K}.\end{aligned}\tag{5.22}$$

Using the local-equilibrium condition, the diffusion equation of the total concentration of colloids reads

$$\partial_t c_{tot} = \nabla(\langle D \rangle c_{tot}) = c_{tot} \nabla \langle D \rangle + \langle D \rangle \nabla c_{tot},\tag{5.23}$$

where $\langle D \rangle = (c_1^{(eq)} D_1 + 2c_2^{(eq)} D_2) / c_{tot}$. Thus we can obtain the thermodiffusion coefficient as $D_T = \nabla_T \langle D \rangle$. Assuming Arrhenius transition rate $K = ke^{\beta \Delta E}$, where $\Delta E = E_2 - E_1$, we can

calculate the thermodiffusion coefficient explicitly

$$S_T \equiv \frac{D_T}{\langle D \rangle} = (E_2 - E_1) (D_2 - D_1) g(\Delta E, T, k, c), \quad (5.24)$$

where $g(\Delta E, T, k, c)$ is a positive-definite function. The sign of the Soret coefficient is determined by the signs of diffusivity difference and the energy difference. According to the Stokes-Einstein relation, the diffusion coefficient is proportional to the inverse of the particle's radius, and the effective radius of a dimer is apparently larger than that of a monomer. Thus, the dimer should diffuse slower, $D_2 - D_1 < 0$. The sign of the diffusivity difference is fixed, then the sign is solely determined by the energy difference. If the slow diffusion state, the dimer, has higher energy, the Soret coefficient will be negative, i.e. the particle favors the hot side. Combining this with the thermophoresis of a single-state particle's positive Soret coefficient can lead to the sign-reverse as a function of temperature.

6 Conclusion

In this work, we discussed the properties of chemical reactions maintained out of equilibrium by non-isothermal conditions.

The aim was to illustrate how non-equilibrium conditions can give rise to the origin of life or, more specifically, the early stages of chemical evolution. For the prebiotic stage of life's formation, we need to study simple reaction systems to see how they gain information from the inhomogeneous environment and evolve to more organized and/or higher-energy states by using negative entropy flux to trigger kinetic stabilization. We showed that even a reaction system of only two states could utilize the non-isothermal condition to maintain itself in an organized state. Within a more complex reaction system, a three-state system, it can dissipate energy between thermal reservoirs of different temperatures to achieve kinetic discrimination of its energy landscape. Only in non-equilibrium conditions do reaction systems show rich properties related to their kinetic features and violate the energetically determined state governed by Boltzmann distribution. Further discussion of dissipation-driven selection is included in our paper[14], in which we extend the three-state system to tree networks and show that the fast-dissipation branch is favored. In Chapter 4, we see how a time-periodic variation of temperature can mimic the temperature gradient to lead to the same dissipation-driven effects on time-average quantities.

Accumulation of chemical reactants in a certain region is essential in prebiotic evolutions and is achieved through thermophoresis[16]. In Chapter 5, we introduce a new mechanism of thermophoresis. As we show, the chemical-state-dependent diffusion coefficient leads to the temperature dependence of effective diffusivity. In the presence of a temperature gradient, the effective diffusivity then shows positional dependence, which finally leads to thermophoresis. This result is first derived for discrete chemical states and then generalized into continuous chemical space. We also discuss that when a particle does not have distinct states for which we can still get thermophoresis by regarding the velocity of a particle as a kind of state. This single-particle contribution can be easily added to the multi-states case. The collective effect of particles is also considered: binding of particles causes the negative Soret coefficient since the binding and unbinding states have different energies and diffusivity. A similar mechanism

has also been found in other non-uniform environments[41–43].

A Appendixes

A.1 Derivation of Langevin equation

The first Hamiltonian is of the molecule, the second one is the environment Hamiltonian and the third part represents the interactions between the molecule and the environment. And the Hamiltonian reads

$$\begin{aligned} H(\mathbf{q}, \mathbf{p}) &= \frac{1}{2} \sum_k \frac{p_k^2}{2M_k} + \frac{1}{2} \sum_k \sum_m V_{mk}(q_k - q_m) \\ H_E(\mathbf{q}^e, \mathbf{p}^e) &= \sum_j \frac{p_j^{e2}}{2m_j} \\ H_{int}(\mathbf{q}, \mathbf{q}^e) &= \sum_k \sum_j V_{mj}^{int}(q_k - q_j^e) \end{aligned} \quad (\text{A.1})$$

For a particle in the environment represented by a pair of coordinates (q_k^e, p_i^e) , the equation of motion reads

$$\frac{d^2}{dt^2}(m_j q_j^e) = -\frac{\partial V_{mj}^{int}}{\partial q_j^e} \quad (\text{A.2})$$

Taking the second order approximation, namely the harmonic oscillator approximation, the interaction between the part of molecular and the solvent molecule j is $V_{mj}^{int} = \omega_{jk}^2 m_j (q_k - q_j^e)^2 / 2$.

$$\frac{d^2 q_j^e(t)}{dt^2} = -\omega_j^2 m_i (q_j^e(t) - \sum_k q_k(t)) \quad (\text{A.3})$$

We assume the solvent molecules move much faster than the molecular coordinates. We can

get the analytical solution of the above equation as

$$q_j^e(t) = q_j^e(0) \cos(\omega_{jk}t) + \frac{p_j(0)}{m_j \omega_{jk}} \sin(\omega_{jk}t) + \sum_k \left(q_k(t) - q_k(0) \cos(\omega_{jk}t) - \int_0^t \frac{p_k(s)}{M_k} \cos(\omega_{jk}(t-s)) \right) \quad (\text{A.4})$$

Plugging it back to the equation of motion of the large molecule

$$\begin{aligned} M_k \ddot{q}_k &= -\frac{\partial \mathcal{H}}{\partial q_k} \\ &= -\frac{1}{2} \sum_m \frac{\partial V_{mk}(q_k - q_m)}{\partial q_k} - \int_0^t \frac{p_k(s)}{M_k} K(t-s) + \xi(t) \end{aligned} \quad (\text{A.5})$$

where

$$\begin{aligned} K(t) &\simeq \sum_{j \in R_k} \omega_{jk} m_j \sin(\omega_{jk}t) \\ \xi(t) &\simeq \sum_{j \in R_k} \omega_{jk}^2 m_j \left((q_j^e(0) - q_k(0)) \cos(\omega_{jk}t) + \frac{p_j^e(0)}{m_j \omega_{jk}} \sin(\omega_{jk}t) \right) \end{aligned} \quad (\text{A.6})$$

Here we applied the assumption that only the solvent molecules close to the k-th component of the large molecule have effective interaction. As shown in Fig 2.1, only the solvent molecules in the dashed circle interact with the k-th part. Thus, the sum in equation (2) does not need to run overall solvent molecules, instead, just the neighboring solvent molecules. And also the k-th component's adjacent molecules do interact with other parts of the large molecule. Therefore we can also drop out the last two terms of $\xi(t)$.

As the solvent molecules are in thermal equilibrium, they should follow the Boltzmann distribution

$$P(\{q_j^e(0), p_j^e(0)\}; \{q_k(0)\}) \propto \exp \left[-\sum_j \left(\frac{p_j^e(0)^2}{2m_j} + \frac{m_j \omega_{jk}^2 (q_j^e(0) - q_k(0))^2}{2} \right) \right] \quad (\text{A.7})$$

Using this probability distribution, we can find the mean and variance of the noise term as

$$\langle \xi(t) \rangle = 0, \quad \langle \xi(t) \xi(t') \rangle = k_B T K(t-t') \quad (\text{A.8})$$

One more thing that needs to clarify is a fast-variable approximation. The solvent particles vibrate much faster than the changing of the momentum of the large molecule, then the

memory damping term $K(t)$ can be approximated by a Dirac delta function.

$$K(t) = 2\gamma_k \delta(t) \quad (\text{A.9})$$

where γ_k is the so-called friction coefficient. The evolution equation of the k -th component of the large particle is

$$M_k \ddot{q}_k = -\partial_{q_k} V(\mathbf{q}) - \gamma_k \dot{q}_k + \xi(t) \quad (\text{A.10})$$

Bibliography

- ¹X. Fang, K. Kruse, T. Lu, and J. Wang, “Nonequilibrium physics in biology”, *Reviews of Modern Physics* **91**, 045004 (2019).
- ²E. Schrödinger, *What is life?: the physical aspect of the living cell, and, mind and matter* (Cambridge University Press, 1944).
- ³W. Martin, J. Baross, D. Kelley, and M. J. Russell, “Hydrothermal vents and the origin of life”, *Nature Reviews Microbiology* **6**, 805–814 (2008).
- ⁴M. S. Dodd, D. Papineau, T. Grenne, J. F. Slack, M. Rittner, F. Pirajno, J. O’Neil, and C. T. Little, “Evidence for early life in earth’s oldest hydrothermal vent precipitates”, *Nature* **543**, 60–64 (2017).
- ⁵U. von Stockar and J.-S. Liu, “Does microbial life always feed on negative entropy? thermodynamic analysis of microbial growth”, *Biochimica et Biophysica Acta (BBA) - Bioenergetics* **1412**, 191–211 (1999).
- ⁶H. C. Fogedby and A. Imparato, “Heat fluctuations and fluctuation theorems in the case of multiple reservoirs”, *Journal of Statistical Mechanics: Theory and Experiment* **2014**, P11011 (2014).
- ⁷H. C. Fogedby and A. Imparato, “A bound particle coupled to two thermostats”, *Journal of Statistical Mechanics: Theory and Experiment* **2011**, P05015 (2011).
- ⁸X. Jin and H. Ge, “Nonequilibrium steady state of biochemical cycle kinetics under non-isothermal conditions”, *New Journal of Physics* **20**, 043030 (2018).
- ⁹R. Pascal, A. Pross, and J. D. Sutherland, “Towards an evolutionary theory of the origin of life based on kinetics and thermodynamics”, *Open Biology* **3**, 130156 (2013).
- ¹⁰R. D. Astumian, “Kinetic asymmetry allows macromolecular catalysts to drive an information ratchet”, *Nature Communications* **10**, 3837 (2019).
- ¹¹M. Baiesi and C. Maes, “Life efficiency does not always increase with the dissipation rate”, *Journal of Physics Communications* **2**, 045017 (2018).
- ¹²A. Pross, “How can a chemical system act purposefully? bridging between life and non-life”, *Journal of Physical Organic Chemistry* **21**, 724–730 (2008).
- ¹³A. Pross and R. Pascal, “How and why kinetics, thermodynamics, and chemistry induce the logic of biological evolution”, *Beilstein Journal of Organic Chemistry* **13**, 665–674 (2017).

- ¹⁴D. M. Busiello, S.-L. Liang, and P. De Los Rios, “Dissipation-driven selection in non-equilibrium chemical networks”, arXiv:1912.04642 [cond-mat, physics:physics] (2019).
- ¹⁵S. Rahav, J. Horowitz, and C. Jarzynski, “Directed flow in nonadiabatic stochastic pumps”, *Physical Review Letters* **101**, 140602 (2008).
- ¹⁶M. Morasch, D. Braun, and C. B. Mast, “Heat-flow-driven oligonucleotide gelation separates single-base differences”, *Angewandte Chemie* **128**, 6788–6791 (2016).
- ¹⁷C. B. Mast, S. Schink, U. Gerland, and D. Braun, “Escalation of polymerization in a thermal gradient”, *Proceedings of the National Academy of Sciences* **110**, 8030–8035 (2013).
- ¹⁸G. W. Ford, M. Kac, and P. Mazur, “Statistical mechanics of assemblies of coupled oscillators”, *Journal of Mathematical Physics* **6**, 504–515 (1965).
- ¹⁹R. Zwanzig, “Nonlinear generalized langevin equations”, *Journal of Statistical Physics* **9**, 215–220 (1973).
- ²⁰K. Sekimoto, *Stochastic energetics*, Lecture Notes in Physics (Springer-Verlag, Berlin Heidelberg, 2010).
- ²¹C. Gardiner, *Stochastic methods: a handbook for the natural and social sciences*, 4th ed., Springer Series in Synergetics (Springer-Verlag, Berlin Heidelberg, 2009).
- ²²G. A. Pavliotis, *Stochastic processes and applications: diffusion processes, the fokker-planck and langevin equations*, Texts in Applied Mathematics (Springer-Verlag, New York, 2014).
- ²³T. L. Hill, “Studies in irreversible thermodynamics IV. diagrammatic representation of steady state fluxes for unimolecular systems”, *Journal of Theoretical Biology* **10**, 442–459 (1966).
- ²⁴J. Schnakenberg, “Network theory of microscopic and macroscopic behavior of master equation systems”, *Reviews of Modern Physics* **48**, 571–585 (1976).
- ²⁵O. Raz, Y. Subaşı, and C. Jarzynski, “Mimicking nonequilibrium steady states with time-periodic driving”, *Physical Review X* **6**, 021022 (2016).
- ²⁶D. M. Busiello, C. Jarzynski, and O. Raz, “Similarities and differences between non-equilibrium steady states and time-periodic driving in diffusive systems”, *New Journal of Physics* **20**, 093015 (2018).
- ²⁷R. D. Astumian, “Stochastic conformational pumping: a mechanism for free-energy transduction by molecules”, *Annual Review of Biophysics* **40**, eprint: <https://doi.org/10.1146/annurev-biophys-042910-155355>, 289–313 (2011).
- ²⁸R. D. Astumian, “Stochastic pumping of non-equilibrium steady-states: how molecules adapt to a fluctuating environment”, *Chemical Communications* **54**, 427–444 (2018).
- ²⁹J. K. Platten, “The soret effect: a review of recent experimental results”, *Journal of Applied Mechanics* **73**, 5 (2006).
- ³⁰M. A. Rahman and M. Z. Saghir, “Thermodiffusion or soret effect: historical review”, *International Journal of Heat and Mass Transfer* **73**, Publisher: Elsevier Ltd, 693–705 (2014).
- ³¹W. Köhler and K. I. Morozov, “The soret effect in liquid mixtures – a review”, *Journal of Non-Equilibrium Thermodynamics* **41**, 151–197 (2016).

- ³²R. Piazza and A. Parola, “Thermophoresis in colloidal suspensions”, *Journal of Physics Condensed Matter* **20** (2008).
- ³³J. Burelbach, D. Frenkel, I. Pagonabarraga, and E. Eiser, “A unified description of colloidal thermophoresis”, *European Physical Journal E* **41**, ISBN: 1292-8941 (2018).
- ³⁴P. Anzini, G. M. Colombo, Z. Filiberti, and A. Parola, “Thermal forces from a microscopic perspective”, *Physical Review Letters* **123**, 028002 (2019).
- ³⁵P. Lançon, G. Batrouni, L. Lobry, and N. Ostrowsky, “Drift without flux: brownian walker with a space-dependent diffusion coefficient”, *Europhysics Letters (EPL)* **54**, 28–34 (2001).
- ³⁶S. Chapman, “On the brownian displacements and thermal diffusion of grains suspended in a non-uniform fluid”, *Proceedings of the Royal Society A: Mathematical, Physical and Engineering Sciences* **119**, 34–54 (1928).
- ³⁷M. Yang and M. Ripoll, “Brownian motion in inhomogeneous suspensions”, *Physical Review E* **87**, 062110 (2013).
- ³⁸M. Yang and M. Ripoll, “Drift velocity in non-isothermal inhomogeneous systems”, *The Journal of Chemical Physics* **136**, 204508 (2012).
- ³⁹T. N. Khazanovich, “On the theory of thermal diffusion in dilute polymer solutions”, *Journal of Polymer Science Part C: Polymer Symposia* **16**, 2463–2468 (1967).
- ⁴⁰A. W. Lau and T. C. Lubensky, “State-dependent diffusion: thermodynamic consistency and its path integral formulation”, *Physical Review E - Statistical, Nonlinear, and Soft Matter Physics* **76** (2007).
- ⁴¹J. Agudo-Canalejo, T. Adeleke-Larodo, P. Illien, and R. Golestanian, “Enhanced diffusion and chemotaxis at the nanoscale”, *Accounts of Chemical Research* **51**, 2365–2372 (2018).
- ⁴²J. Agudo-Canalejo, P. Illien, and R. Golestanian, “Phoresis and enhanced diffusion compete in enzyme chemotaxis”, *Nano Letters* **18**, 2711–2717 (2018).
- ⁴³J. Agudo-Canalejo, P. Illien, and R. Golestanian, “Cooperatively enhanced reactivity and “stabilitaxis” of dissociating oligomeric proteins”, *Proceedings of the National Academy of Sciences* **117**, 11894–11900 (2020).